Running head:
Spatio-Temporal Actions of Seed Pectin Methylesterases

Corresponding author:
Gerhard Leubner-Metzger
School of Biological Sciences,
Plant Molecular Science and Centre for Systems and Synthetic Biology,
Royal Holloway, University of London,
Egham, Surrey, TW20 0EX, United Kingdom
Web: 'The Seed Biology Place', www.seedbiology.eu
Email: Gerhard.Leubner@rhul.ac.uk
Phone: ++44 1784 443553
Fax: ++44 1784 414224

PLANTPHYSIOL/2014/247429 - revised version

Journal Research Area: Genes, Development and Evolution

Promotion of Testa Rupture during *Lepidium sativum* Germination Involves Seed Compartment-Specific Expression and Activity of Pectin Methylesterases [W][OPEN]

Claudia Scheler[2], Karin Weitbrecht[2], Simon P. Pearce[2], Anthony Hampstead, Annette Büttner-Mainik, Kieran J. D. Lee, Antje Voegele, Krystyna Oracz, Bas J. W. Dekkers, Xiaofeng Wang, Andrew T. A. Wood, Leónie Bentsink, John R. King, J. Paul Knox, Michael J. Holdsworth[3], Kerstin Müller[3], and Gerhard Leubner-Metzger[3*]

Botany / Plant Physiology, Institute for Biology II, Faculty of Biology, University of Freiburg, Schänzlestr. 1, D-79104 Freiburg, Germany (C.S., K.W., A.B-M., K.O., G.L-M.);
Helmholtz Zentrum München, Deutsches Forschungszentrum für Gesundheit und Umwelt (GmbH), Ingolstädter Landstr. 1, D-85764 Neuherberg, Germany (C.S.);
Staatliches Weinbauinstitut Freiburg, Merzhauserstr. 119, D-79104 Freiburg, Germany (K.W.);
Centre for Plant Integrative Biology, School of Biosciences, University of Nottingham, Sutton Bonington Campus, Loughborough, Leices, LE12 5RD, United Kingdom (S.P.P., J.R.K.);
School of Mathematical Sciences, The University of Nottingham, Nottingham, NG7 2RD, United Kingdom (S.P.P., A.H., A.T.A.W., J.R.K.);
Agroscope, Institute for Plant Production Sciences, Seed Quality, Reckenholzstrasse 191, CH-8046 Zürch, Switzerland (A.B.-M.);
Centre for Plant Sciences, Faculty of Biological Sciences, University of Leeds, Leeds LS2 9JT, United Kingdom (K.J.D.L., J.P.K.);
NIHR Trainees Coordinating Centre, Leeds Innovation Centre, 103 Clarendon Road, Leeds LS2 9DF, United Kingdom(K.J.D.L.);
School of Biological Sciences, Plant Molecular Science and Centre for Systems and Synthetic Biology, Royal Holloway, University of London, Egham, Surrey, TW20 0EX, UK; www.seedbiology.eu (A.V., G.L.-M.);
Department of Plant Physiology, Warsaw University of Life Sciences - SGGW, Nowoursynowska 159, 02-776, Warsaw, Poland (K.O.);
Wageningen Seed Laboratory, Laboratory of Plant Physiology, Wageningen University and Research Centre, NL-6708 PB Wageningen, The Netherlands (B.J.W.D., L.B.);
College of Life Sciences, South China Agricultural University, Guangzhou 510642, China (X.W.);
Division of Plant and Crop Science, School of Biosciences, University of Nottingham, Sutton Bonnington LE12 5RD, United Kingdom (S.P.P., M.J.H., K.M.);

Laboratory of Growth Regulators, Faculty of Science, Palacký University and Institute of Experimental Botany AS CR, v.v.i., Šlechtitelů 11, CZ-783 71, Olomouc, Czech Republic (G.L.-M.)

Footnotes

[1] Our work was funded by the ERA-NET Plant Genomics vSEED project through grants from the Deutsche Forschungsgemeinschaft (grant no. DFG LE720/8) to G.L.-M. and from the UK Biotechnology and Biosciences Research Council to J.P.K. (grant no. BB/G024898/1) and M.J.H.&J.R.K. (grant no. BBG02488X1) and the Netherlands Organization for Scientific Research to L.B. (grant no. 855.50.011), as well as by grants from the Deutsche Forschungsgemeinschaft (grant no. DFG LE720/6) and Wissenschaftliche Gesellschaft Freiburg to G.L.-M., the Guangdong Natural Science Fundation (grant no. 07006658) to X.W., a Marie Curie IOF fellowship to K.M., and an Alexander von Humboldt-foundation Research Fellowship to K.O.. J.R.K additionally acknowledges the support of the Royal Society and the Wolfson Foundation.

[2] These authors contributed equally to the article

[3] These authors contributed equally to the article

PLANTPHYSIOL/2014/247429 - revised version

* Address corresponce to: Gerhard Leubner-Metzger; Email Gerhard.Leubner@rhul.ac.uk; Web 'The Seed Biology Place' – www.seedbiology.eu

The author responsible for distribution of materials integral to the findings presented in this article in accordance with the policy described in the Instructions for Authors (www.plantphysiology.org) is: Gerhard Leubner-Metzger (Gerhard.Leubner@rhul.ac.uk)

[W] The online version of this article contains Web-only data.
[OPEN] Articles can be viewed online without a subscription.
www.plantphysiology.org/cgi/doi/10.1104/pp.XXX.XXXXXX

Running title: Seed Pectin Methylesterases

Abstract

Pectin methylesterase (PME) controls the methylesterification status of pectins and thereby determines the biophysical properties of plant cell walls, which are important for tissue growth and weakening processes. We demonstrate here that tissue-specific and spatio-temporal alterations in cell wall pectin methylesterification occur during the germination of *Lepidium sativum*. These cell wall changes are associated with characteristic expression patterns of PME genes and resultant enzyme activities in the key seed compartments CAP (micropylar endosperm) and RAD (radicle plus lower hypocotyl). Transcriptome and RT-qPCR analysis as well as PME enzyme activity measurements of separated seed compartments, including CAP and RAD, revealed distinct phases during germination. These were associated with hormonal and compartment-specific regulation of PME group 1, PME group 2, and PME inhibitor (PMEI) transcript expression and total PME activity. The regulatory patterns indicated a role for PME activity in testa rupture (TR). Consistent with a role for cell wall pectin methylesterification in TR, treatment of seeds with PME resulted in enhanced testa permeability and promoted TR. Mathematical modelling of transcript expression changes in germinating *L. sativum* and *Arabidopsis thaliana* seeds suggested that group 2 PMEs make a major contribution to the overall PME activity rather than acting as PME inhibitors. It is concluded that regulated changes in the degree of pectin methylesterification through CAP and RAD specific PME and PMEI expression play a crucial role during Brassicaceae seed germination.

Mature seeds of members of the Brassicaceae family such as *Arabidopsis thaliana* ('Arabidopsis') and *Lepidium sativum* (garden cress) are endospermic, i.e. the embryo is surrounded by a thin living cell layer, the endosperm, and a dead outer layer, the testa. Many angiosperm seeds, including those of *L. sativum* and Arabidopsis, germinate in a two-step process: After the initial phase of water uptake by the dry seeds (imbibition), testa rupture (TR) occurs, and is subsequently followed by endosperm rupture (ER) which marks the completion of germination (Liu et al., 2005; Müller et al., 2006). Germination is controlled by two opposing forces, the increasing growth potential of the radicle, and the resistance of the testa and endosperm tissues covering it (Bewley, 1997; Schopfer, 2006; Linkies and Leubner-Metzger 2012). After TR, endosperm resistance decreases through tissue softening, a process called endosperm weakening (Müller et al., 2006; Linkies et al., 2009). Both radicle elongation and endosperm weakening require cell wall modifications (Schopfer, 2006; Müller et al., 2009; Morris et al. 2011).

Plant cell walls are the main determinants for the shape and biomechanical properties of plant tissues, organs, and even the whole plant body. They control turgor-driven water uptake to allow cell growth through changes in extensibility, which depend on wall composition and the interaction between their components (Cosgrove and Jarvis, 2012; Thompson, 2005; Yoshida et al, 2014). One of the most abundant groups of polysaccharides in primary cell walls are pectins. Pectins are complex polysaccharides that are characterized by α-1,4-linked galacturonic acid (Mohnen, 2008; Tan et al., 2013), and are present in the middle lamellae, and are key polymers in cell separation processes. The most abundant plant cell wall pectin is homogalacturonan (HG). HG is a linear polymer of (1,4)-linked-α-D-galacturonic acid which can be modified by methylesterification at the C-6 carboxyl position to form methylesterified HG (Me-HG) (Wolf et al., 2009a). The degree of methylesterification is variable between developmental stages, tissues, and even regions of the wall of an individual cell, and strongly affects the mechanical properties of cell walls (Braybrook et al., 2012). After synthesis in the endomembrane system, HG is secreted in a highly methylesterified form into the plant cell wall of growing cells (Mohnen, 2008).

Pectin methylesterases (PME) (EC 3.1.1.11) catalyze the demethylesterification of HG (Wolf et al., 2009a). PMEs are ubiquitous cell wall-associated enzymes that are found in all higher plants, as well as in some bacteria and fungi. PMEs can act linearly to de-esterify stretches of Me-HG to give rise to blocks of free carboxyl groups which can be cross-linked by calcium ions. These calcium bridges influence cell wall porosity and may enhance overall firmness of tissues. PMEs can also act in a non-linear fashion and de-esterify only individual galacturonate residues or short stretches, which does not allow for calcium bridges to form, leading to a looser cell wall matrix structure. PME activity might promote subsequent action

of cell wall hydrolases such as endo-polygalacturonases (PG) (Wakabayashi et al., 2000 and 2003), which contribute to cell wall weakening and/or cell separation (Gonzalez-Carranza et al., 2007). PMEs have been shown to be involved in pectin remodeling at different developmental stages: e.g. pollen tube growth (Eckardt, 2005), root elongation and its reaction to soil aluminium concentrations (Yang et al., 2013), hypocotyl elongation (Pelletier et al., 2010), fruit ripening (Hyodo et al., 2013) and seed germination (Müller et al., 2013). PMEs are encoded by a large multigene family which has been classified into two groups (Wang et al., 2013): All PMEs have a conserved pectinesterase domain (Pfam01095), but only group 2 has in addition a PME inhibitory domain (Pfam04043). PME activity is regulated by PME inhibitor proteins (PMEI) (Giovane et al., 2004; Wolf et al., 2009a).

In our integrative study we discovered that during the seed germination of *L. sativum* changes in transcript abundances of specific PMEs and PMEIs are reflected in seed compartment-specific changes in PME activity, and accompanied by spatio-temporal changes in cell-wall pectin methylesterification. We mathematically modelled the contribution of the different groups of PMEs and of PMEIs to the degree of methylesterification in the *L. sativum* seed cell walls. Based on these molecular, physiological, histochemical and biophysical analyses we propose that PME activity is involved in the germination process of *L. sativum*, and is differentially regulated in a spatial and temporal manner.

RESULTS

Seed compartment specific transcriptome analysis of *Lepidium sativum* germination

We utilised the fact that *L. sativum* has a two step germination process, with testa rupture (TR) and endosperm rupture (ER) separated by several hours, to conduct a dense spatio-temporal transcriptome analysis during the germination process (Fig. 1). We investigated transcriptome changes in the seed compartments that are directly involved in ER, the micropylar endosperm (CAP, Fig. 1B) and the radicle with the lower part of the hypocotyl (RAD; embryo growth zone, Fig. 1B), at key timepoints during the germination process from early imbibition to completion of ER (Fig. 1A and B). At the timepoints when ca. 50% of the seed population had reached TR and ER, respectively, we divided the sampling population between the seeds that had already undergone rupture (+TR or +ER) and those that had not (-TR or -ER), so that we could compare e.g. samples that would have undergone TR within the next hour or two with those that already had a ruptured testa. We also sampled cotyledons (COT) and non-micropylar endosperms (NME) at three timepoints (Fig. 1). Seed compartment-specific gene expression analysis for *L. sativum* have been successfully performed before (Linkies 2009) using CATMA spotted PCR-amplified gene-specific tag

(GST)- based microarrays, but only for a small number of samples that allowed for a limited analysis of the *L. sativum* FR1 germination process. Our sampling concept in this work with *L. sativum* FR14 (Fig. 1) led to a time course with sufficient spatio-temporal resolution to investigate the distinct phases of germination and make physiological relevant comparisons.

We performed microarrays by hybridising *L. sativum* RNA to Affymetrix ATH1 microarrays designed for Arabidopsis. Heterologous microarrays on Arabidopsis ATH1 chips have been successfully employed by several groups to elucidate transcriptome changes in un-sequenced Brassicaceae species or in species without commercially available microarrays (Hammond et al., 2006; Slotte et al., 2007). To further improve the method for *L. sativum* we developed a sophisticated masking approach that allowed us to extract a maximum of information from the arrays (see methods). Using the masking method presented here, with a False Discovery Rate of 0.01, 36.6% of probes and 65.1% of probesets were retained, leading to 5793 genes identified as being differentially expressed between 1 hour after sowing and 16 hours after sowing in the CAP, and 6098 genes in the RAD. Conversely, using the method of (Hammond et al., 2005) the maximal number of differentially expressed genes was 1712 at a cutoff of 100. Thus our method retained a much larger number of differentially expressed genes that could then be used for further analysis. Normalized expression values for *L. sativum* were therefore obtained for 13895 transcripts (Supplemental Data Set 1); with *L. sativum* gene transcripts referring to the putative Arabidopsis orthologs defined by having an Arabidopsis Genome Initiative (AGI) identifier such as At1g62380. The Supplemental Data Sets 2 and 3 provide the normalised $\log_2$ values for the mean and SD expression results, respectively.

Seed compartment-specific differentially regulated *Lepidium sativum* transcriptome during germination shows overrrepresentation of cell wall related transcripts at the TR stage transition

A principal component analysis (PCA) shows the general distribution of values calculated into *eigenvectors* and makes it possible to identify the eigenvectors with the greatest influence on sample variance. In our arrays the *eigenvectors* with the biggest influence appear to correspond to time and seed compartment (Fig. 1c). In dry seeds and at 1 h after sowing, RAD and CAP samples still cluster together, separating from 3 h after sowing. In the RAD distinct clusters formed at the phase transition time point at 7 h, where we segregated for -TR and +TR , and at 16 h, where we segregated for seeds that had undergone ER and thus completed the germination process (+ER), and those whose endosperm had not ruptured yet (-ER). The same was true for the CAP at 7 h (+TR versus -TR), although the 16 h CAP with ER clusters with the CAP samples without ER.

The COT samples exhibited a higher variance throughout the time course (Fig. 1). The NME for the two time points without TR clustered apart from the CAP samples, but was still closer to them than to the RAD and COT samples derived from the embryo. At 13 h, the NME samples varied more and clustered closer still to the CAP samples (Fig. 1). The finding that transcriptomes differ between the distinct seed compartments and over time is further supported by a cluster analysis of the transcript abundance patterns which showed five clearly distinct clusters (Supplemental Fig. S1). Together with the PCA analysis (Fig. 1) it supports the view that testa rupture is a decisive step during the germination process which is associated with abundant transcriptomes changes (+TR versus -TR) in both the CAP and the RAD.

The Genome Ontology (GO) over-representation analyses of the TR rupture transition time point (Supplemental Tables S1 and S2) indicate that both hormone regulation and cell wall modifications are overrepresented in the differentially regulated transcripts in the different seed compartments. We decided to look in more detail at pectin methylesterases (PME) and PME inhibitor proteins (PMEI), as those cell wall modifying enzymes and inhibitors have been shown to be tied in with hormonal regulations and to play a role in seed germination of Arabidopsis (Müller et al., 2013; Saez-Aguayo et al., 2013), and pectinesterase activity and inhibition was one of the activities whose GOs were specifically overrepresented in the RAD (Supplemental Table 2).

Spatio-temporal patterns of HG and Me-HG pectin cell wall epitopes during *Lepidium sativum* seed germination

In order to observe if, where and at which stage during the *L. sativum* seed germination process changes in the degree of pectin methylesterification actually happen in the RAD and CAP, we studied HG epitopes *in situ*. To distinguish pectic HG in its methylesterified form (Me-HG) from the de-methylesterified form (HG) we used a set of well characterized monoclonal antibodies (Clausen et al. 2003; Verhertbruggen et al. 2009) in conjunction with fluorescence imaging (Fig. 2). Antibody LM19 is specific for de-methylesterified HG (dHG) and its epitope was detected in seeds 3 h after sowing. The LM19 epitope was ubiquitously distributed in the cell walls of the RAD, as well as in the CAP ('E' in Fig. 2), the testa and the testa-derived mucilage layer. In contrast, the JIM7 (Fig. 2) and LM20 (not shown) Me-HG epitopes were restricted to the testa and mucilage and were present at reduced levels in the RAD, but absent from the CAP. The pattern of the LM19 HG epitope did not change between our sampling times. However, the spatial distribution of Me-HG (JIM7) was altered. The JIM7 signal increased in the RAD and appeared in the inner cell wall of the CAP upon TR (Fig. 2). This suggests that there is new deposition of pectin into the cell wall, as HG is

methylesterified in the Golgi and secreted as Me-HG. In testa and mucilage, the JIM7 epitope was detectable in all phases during seed germination (Fig. 2).

Molecular phylogenetic analyses of *Arabidopsis thaliana* and *Lepidium sativum* PMEs and their inhibitors

We mined our microarrays for the expression patterns of putative PMEs and PMEIs in *L. sativum* seeds (Supplemental Data Sets 1 to 3). As the *L. sativum* genome has not been sequenced, we started by identifying 136 Arabidopsis sequences for PMEs and PMEIs by annotation and similarity searches in public databases, with subsequent verification of the existence of specific domains in the predicted proteins. According to our molecular phylogenetic analysis of their full-length predicted protein sequences, these Arabidopsis PMEs and PMEIs cluster into three large groups (Fig. 3): group 1 PME (22 members) and group 2 PME (45 members) contain the PME domain (Pfam01095) which harbors five characteristic sequence motifs important for PME activity. The group 2 PMEs additionally possess a PMEI domain (Pfam04043) with conserved cysteines, and both domains are separated by a processing motif (PM) that is a putative target for subtilisin-like proteases. The third cluster consists of 69 PMEIs (Fig. 3).

We used the seed-specific eFP-browser and the eNorthern tool at www.bar.utoronto.ca (Winter et al., 2007) for an *in silico* analysis of the PME/PMEI transcript expression patterns in imbibed whole Arabidopsis seeds (Fig. 3). This analysis yielded a general pattern in which many PME group 2 transcripts are down-regulated by cold stratification ('1' in Fig. 3). However, a small number of group 2 PME and PMEIs was strongly upregulated during the first few hours of the germination process ('2' in Fig. 3). PMEs from both groups as well as PMEIs are upregulated in the course of the germination process in the presence of abscisic acid (ABA) ('3' in Fig. 3).

We then compared the expression of PME and PMEI transcripts that we identified in our arrays for *L. sativum* seeds (4 group 1 PMEs, 28 group 2 PMEs, 25 PMEIs) in CAP and RAD (Fig. 4) with their homologs in Arabidopsis (data extracted from the transcriptome of Dekkers et al., 2013) as defined by the transcripts that bind to the same probesets. There was an overall stronger differential regulation visible in the Arabidopsis data, which may be due to the heterologous nature of the *L. sativum* arrays or to the fact that the Arabidopsis seed compartments were less confined and contained additional tissues (Fig. 4). However, we could clearly observe that the genes that were strongly differentially regulated in *L. sativum* seed compartments were also strongly regulated in Arabidopsis in a similar manner in the same compartments (Fig. 4).

PME activity in *Lepidium sativum* seed compartments in relation to TR and ER

With the large number of PMEs and PMEIs and their diverse expression patterns, it is hard to predict whether there is a net PME activity at any given stage and seed part, and how it changes over the course of germination. We therefore measured the total PME activity in *L. sativum* RADs and CAPs. The total PME enzyme activity was roughly 10-fold higher in the CAP compared to the RAD during *L. sativum* seed germination (Fig. 5). The PME activities in the CAP were highest during imbibition and in the very early phase of germination (3-8 h), declined around the time of TR, then stabilised at a lower activity as the population reached the completion of TR followed by ER (16 h) (Fig. 5A). The activity in the RAD also decreased around TR, but then increased again as the seeds neared ER, and peaked at a stage where the whole population had reached TR, but not progressed to ER yet (16 h).

Endosperm weakening and rupture of *L. sativum* are known to be delayed by exogenous ABA, while the kinetics of TR is unaffected by its presence. In accordance with this, when ABA was added to the germination medium, the population only completed ER after about 70 h, but the timing of TR did not change significantly (Fig. 5B). PME activity in the CAP during the early germination phase before TR was similar in seed populations with and without ABA. However, when this seed population neared its delayed ER, PME activity was significantly lower than at the physiologically equivalent time point without ABA (Fig. 5B). PME activity in the RAD was relatively constant over time, and ca. 2-fold lower in the ABA-series compared to the control (Fig. 5B).

Mathematical model of PME activity in the *Lepidium sativum* CAP and RAD

As mentioned above, PMEs fall into two groups, one of which (group 2) contains a PMEI domain. In order to explore the significance of the two PME groups, along with the action of the PMEIs, on the total PME activity and therefore to the pectin de-methylesterification process, we constructed a biologically informed network of reactions (Fig. 6A) and converted it into a system of ordinary differential equations (ODEs). Cumulative transcript accumulation for each PME group (Fig. 6B) was used as proxy for their protein accumulation. The network (Fig. 6) that was used as a basis for our set of ODEs centres on the demethylesterification of MeHG, caused by either of the PME groups, with PMEI inhibiting both groups of PMEs and group 2 PMEs able to inhibit themselves. Several assumptions were made to simplify the system for the purpose of modelling: 1) Spatial variations are neglected; 2) negligible deposition of additional pectin occurs over the timescale of interest (germination process until ca. 16h); 3) interactions between PME proteins with their inhibitors irreversibly remove the proteins from the system; 4) protein-production rates are proportional to the levels of the relevant mRNA, the latter being obtained from the transcriptomic data; 5) a group 2 PME

327 molecule is able to inactivate itself, since it contains both the PME and PMEI domains. These
328 assumptions and the network (Fig. 6A) lead to equations 1-8 (Fig. 6C), see Materials and
329 Methods for further explanation. The model was fitted to the PME enzyme data shown in Fig.
330 5A, with the resulting parameters listed in Supplemental Table S3. The resulting PME activity
331 predicted by the model after fitting is shown in Fig. 6D in comparison to the measured PME
332 enzyme activity data.
333 PME and PMEI cumulative transcript accumulation within *L. sativum* seed compartments, our
334 proxy for protein production, appears to be phasic in both CAP and RAD (Fig. 6B): first the
335 group 1 PMEs are produced, then the PMEI proteins and finally the group 2 PMEs. This is
336 especially striking in the RAD, since the group 2 PMEs do not have the same escalation in
337 the CAP, where group 2 PME production peaks around the time of TR before declining.
338 Parameter sensitivity analysis was carried out on the model, and it was noted that altering
339 the activating reaction rates, α_i, has a greater impact on the model than varying the inhibiting
340 reaction rates, ζ_i. Our parameter (Supplemental Table S3) sensitivity analysis therefore gives
341 insight into which processes are most significant in governing the overall activity and open
342 the way for subsequent application of the model and for its refinement.
343 Our mathematical model implies that inhibiting processes, in particular by the group 2 PMEs,
344 are less important for the overall activity than their de-methylesterification function. This
345 suggests that the primary importance of the group 2 PMEs is in their PME action rather than
346 their PMEI behaviour (see discussion). Analysing group 2 PME expression pattern (see next
347 section) is therefore relevant to PME enzyme activity pattern (Fig. 5).
348
349 **Hormonal and seed-compartment specific regulation of *Lepidium sativum* group 2**
350 **PMEs**
351 With the large number of differentially regulated group 2 PME (Fig. 4) in our arrays for both
352 RAD and CAP, as well as the insight from the model (Fig. 6) that the group 2 PMEs are
353 predicted to play a role mostly as PMEs and not as inhibitors, we decided to clone and look
354 in detail at several *L. sativum* group 2 PMEs (Fig. 7). Several group 2 PMEs were
355 dramatically up-regulated in whole Arabidopsis seeds (Fig. 3): *At1g11580* increased >100-
356 fold, but we did not obtain data corresponding to this transcript from our heterologous array
357 analysis. *At2g26440* and *At3g14310* were >100-fold up-regulated during the first 24 h of
358 imbibition in Arabidopsis, but did not show changes in the *L. sativum* arrays in either seed
359 compartment under the conditions we used for our arrays.
360 We fully cloned and analysed the cDNAs for the *L. sativum* PME group 2 homolog of
361 Arabidopsis *At1g11580*, which we named *LesaPME11580*. All other cloned *L. sativum* PME
362 cDNAs were named following the same principle, including PME group 2 *LesaPME26440*,

LesaPME14310, and *LesaPME51490* (Supplemental Table S4). Taken together, the sequence comparisons (for details see Supplemental Fig. S2) considering known domains (Markovic and Janecek, 2004; Pelloux et al., 2007) strongly suggest that *LesaPME11580* is a functional PME group 2 of *L. sativum*. We also cloned the full length cDNA of *LesaPMEI14890*, which shows the typical PMEI domain and other characteristic features of this class of inhibitors (Supplemental Fig. S2), and is therefore most likely a functional PMEI.

Using qRT-PCR we analysed the transcript expression of the *L. sativum* group 2 PMEs (Fig. 7) and a small selection of group 1 PMEs and PMEIs (Supplemental Fig. S3) in the CAP and RAD with and without exposure to ABA. *In vitro* PME activities were measured in the CAP and RAD at two sampling time points - seeds that had just undergone TR ("early - 0% ER"), and seeds just before ER ("late - 50% ER") - for the control and for the ABA treatment (Fig. 7A). In all conditions tested, PME activity in the RAD was significantly lower than in the CAP. In both seed compartments, ABA inhibited PME activity compared to the untreated control (Fig. 7A). Supplemental Figure S3 contains additional data for exposure to ACC, the precursor of the plant hormone ethylene which acts antagonistically to ABA in the germination process of *L. sativum* (Linkies et al., 2009). ACC had no effect on total activity in the presence or absence of ABA in the RAD, but led to a strong increase in activity in the CAP at the TR time point (Supplemental Fig. S3).

All transcripts we investigated showed a response to ABA that differed between RAD and CAP, confirming the importance of investigating the seed compartments separately. *LesaPME11580* was expressed more abundantly in the RAD compared to the CAP (Fig. 7B). The transcript stayed at the same level at the two time points we investigated in the RAD, but declined in the CAP between the early and late time point. Treatment with ABA down-regulated *LesaPME11580* in all conditions tested and in both seed compartments (Fig. 7B), while ACC only caused a down-regulation in the CAP and not in the RAD (Supplemental Fig. S3). *In situ* mRNA hybridization (Supplemental Fig. S4) confirmed that *LesaPME11580* transcripts localized to the RAD, and were hardly detectable in the CAP. *LesaPME26440* was also predominantly expressed in the RAD (Fig. 7C), but contrary to *LesaPME11580* was down-regulated in the presence of ABA specifically at the early time point in the CAP and the late time point in the RAD. In addition, its abundance in the CAP was lower at the later time point then it was at the early time point. *LesaPME51490* showed a predominant expression in the CAP (Fig. 7D) while *LesaPME14310* (Fig. 7E) was expressed in both seed compartments at a low level. *LesaPME14310* expression was sensitive to ABA in the medium only at the late time point in the RAD, whereas ABA had no effect on *LesaPME14130* at the other time points. Compared to the four group 2 PMEs that we

investigated, the group 1 *LesaPME29090* transcript abundance was around 10-fold higher, and there was no appreciable down-regulation by ABA (Supplemental Fig. S3).

Exogenous treatment with PME enhances testa permeability and promotes testa rupture

Having investigated the endogenous PME transcript abundances, activities and pectin methylesterification patterns in the *L. sativum* CAP and RAD during germination, we focused on the question if treatment of seeds with exogenous PME affects their germination. Interestingly, addition of 0.2 U orange peel PME to the seed incubation medium (0.03 U PME /ml) promoted their TR (Fig. 8A) but did not appreciably affected ER (Supplemental Fig. S5A). In contrast relatively high PME amounts (ca. 20 U) delayed TR and ER (Supplemental Fig. S5). Earlier work (Linkies et al. 2009) showed that while treatment of *L. sativum* seeds with ABA or the ethylene precursor ACC affected ER, it did not affect the kinetics of TR. Addition of 0.2 U PME plus ABA or ACC to the seed incubation medium also promoted TR (Fig. 8A) which suggests that the PME action is a direct effect of the enzyme action and could be associated with an increased testa and/or mucilage permeability.

To assay for testa permeability we imbibed seeds in tetrazolium assay solution, a method used to analyse Arabidopsis *transparent testa* mutants (Debeaujon et al., 2000) and the effect of myrigalone on *L. sativum* seeds (Voegele et al., 2012). We imbibed *L. sativum* seeds in tetrazolium salt solution in the absence (CON) or presence of 0.2 U PME, thus at a concentration of PME that led to earlier TR. After 9 h, the embryos were excised from the seeds, photographed and categorized (Fig. 8B). For CON 88% of the embryos were unstained, i.e. the testa was impermeable to the dye, and 12% were yellow, showing a low staining intensity which indicates that the low testa permeablility. Thus, the testa permeability of CON-imbibed seeds for tetrazolium salts was very low. In contrast, for seeds treated with 0.2 U PME, only 46% of the embryos were pale (impermeable) and 20% stained yellow (low permeability), while 34% stained partly (either at the cotyledon base or the radicle tip) or almost fully red (highly permeable) (Fig. 8B and Supplemental Fig. S6).

PME-mediated de-methylesterification of Me-HG increases the cell wall HG content. Polygalacturonase (PG) is a pectin degrading enzyme that cleaves the α-1,4-D-galacturonosidic linkages of HG chains. Concerted action of PME and PG is therefore known to cause extensive pectin depolymerization (Wakabayashi et al., 2000 and 2003). We therefore assumed that, if testa and mucilage permeability depend on the state of pectin, PG should further enhance the testa permeability when exogenously applied in combination with 0.2 U PME. This was indeed the case, only 18% of the embryos were pale (impermeable), 20% were stained yellow and 62% were stained partly or almost fully red upon treatment with

PME plus PG (Fig. 8B and Supplemental Fig. S6). We conclude that the promoting effect on TR and ER by low concentrations of PME is at least partially achieved through an enhanced permeability of the testa and/or mucilage layer (Fig. 8).

DISCUSSION

Testa rupture constitutes a transition between phases of gene expression and enzyme activities in the *Lepidium sativum* CAP and RAD

Our microarray analysis provides a high-resolution picture of seed-compartment specific transcriptome changes during *L. sativum* seed germination. The added density of sampling time points made possible by this technical advance supports the identification of the importance of TR as a transitional event during *L. sativum* seed germination. Many transcripts showed an increase in abundance shortly before or more often just after the TR event. One group of genes strongly up-regulated around TR are cell wall modifying enzymes, and cell wall related genes were evident in our GO overrepresentation analysis. This indicates the importance of cell wall remodeling in the CAP and RAD around and after the time of TR. This increased level of expression is then maintained or further increased for the remaining germination process. While specific groups of genes such as the cell-wall modifying enzymes are up-regulated at TR, the overall number of differentially regulated genes drastically drops once TR is complete. These observations fit with those made using microarrays with seed-compartment specific RNA of Arabidopsis, where testa rupture also emerged as a central event for transcriptional regulation in Arabidopsis seeds (Dekkers et al., 2013). The transitional nature of the TR time point was also evident in our principal component analysis (Fig. 1): up to and including TR, the CAP and NME endosperm samples are clearly distinguishable but after TR from 10 to 16 h with and without ER the samples cluster together as one group.

As TR is not influenced by the presence of ABA in the germination medium, but ER is strongly delayed by ABA, the processes that begin at TR are clearly subject to further hormonal regulation once they have been initiated (Linkies et al., 2009). For cell wall modifying enzymes, this has been observed for PME enzyme activities during Arabidopsis seed germination (Müller et al., 2013). Whole seed total PME activity increased until TR was reached and then declined. When ABA was added to the medium, TR still constituted the highest point of PME activity, but the activity only decreased with a delay after a plateau phase (Müller et al., 2013).

Cell wall modifying enzymes are differentially regulated at the time of testa rupture in *Lepidium sativum* in a seed-compartment specific manner

Cell wall modifications are necessary to allow radicle elongation and endosperm weakening, the two processes that eventually lead to ER (Schopfer, 2006; Linkies et al. 2012). It is also possible that cell wall modifications contribute to testa rupture, as a cell wall loosening in the RAD and CAP and a subsequent volume increase through water uptake could provide the additional force necessary to overcome the breaking resistance of the testa. The testa is dead tissue, but cell wall modifying enzymes could be secreted from the underlying endosperm to cause modifications in the inner testa cell walls which could lead to site-specific weakening. A number of cell wall modifying genes, and the enzyme activities of their products, have been shown to be differentially regulated before ER in the seeds of various endospermic species, e.g. beta-1,3-glucanase in tobacco (Leubner-Metzger et al, 2005), beta-1,4-mannanase in tomato (Nonogaki et al., 2000), *L. sativum* (Morris et al. 2010) and Arabidopsis (Iglesias-Fernandez et al., 2011), and xyloglucan endo-transglycosylases/hydrolases in *L. sativum* (Voegele et al. 2011; Graeber et al. 2014) and Arabidopsis (Endo et al., 2012), and species-specific changes in cell wall composition have been observed during the later germination process (Lee et al., 2012), supporting the importance of the cell wall remodelling during seed germination.

We found that PME activity during germination was an order of magnitude higher in the CAP than in the RAD. A higher activity in the seed covering layers than the radicle was also observed in germinating seeds of the conifer yellow-cypress (*Chamaecyparis nootkatensis*, formerly yellow cedar) (Ren and Kermode, 2000). We observed the highest PME activity in the CAP in the first hours after the start of imbibition (Fig. 5A), which possibly prevents preterm CAP weakening, similar to the observation by (Müller et al., 2013) that high PME activity in whole seeds was associated with a delay of ER in Arabidopsis. Contrary to the CAP, the RAD showed an increase of PME activity only after TR.

Our modelling approach (Fig. 6) that used the CAP and RAD-specific PME activities we measured as well as the compartment-specific transcriptomes predicted that group 2 PMEs, although they possess a PMEI domain, mainly contribute their PME activity rather than an inhibitory effect on themselves or other PMEs to the overall PME activity in the distinct seed compartments. Beyond seed, our mathematical modelling provides support with a completely independent apporach for the experimental evidence provided by others (Wolf et al., 2009b) that the PMEI domains of group 2 PMEs are cleaved off during protein maturation and thus not active as inhibitors.

Changes in pectin methylesterification around TR might account for transcriptome changes through mechanosensing processes

In situ analyses indicated that de-esterified HG was present throughout the *L. sativum* seed cell walls during the whole germination process, and was particularly abundant in the seed covering layers indicating that PMEs are widely active in seed cell walls. Me-HG epitopes were only detected in the CAP around the time of TR. It is likely that this indicates the addition of new cell wall material in the endosperm, as there is currently no known mechanism by which methylester groups can be added to HG *in muro*. The fact that there are changes in PME activity as well as in the degree of methylesterification around the time of TR suggest that this contributes to the biomechanical changes which ultimately lead to ER (Linkies et al., 2009; Martínez-Andújar et al., 2012; Dekkers et al., 2013). It has been shown that changes in elasticity caused by changes in pectin methylesterification in the apical meristem are crucial for phyllotaxis (Peaucelle et al., 2011; Braybrook and Peaucelle, 2013). PME action has also been connected with brassinosteroid signaling, as several of the strong phenotypes caused by overexpression of AtPMEI5 could be suppressed when a brassinosteroid receptor was mutated in the overepressor (Wolf et al., 2012). Brassinosteroids are also known to promote germination in Arabidopsis (Steber, 2001) and tobacco (Leubner-Metzger 2001), thus a change in their signalling caused by regulation on PME activity might contribute to changes in germination behaviour.

Exposure to PMEs changes seed coat permeability and germination speed

Low levels of exogenous PME promoted TR and ER, while it was delayed by higher PME concentrations (Fig. 8). The opposing effects of different concentrations of PME might result from differences in the degree and pattern of de-methylesterification caused by the different concentrations. It is possible that low PME concentrations accelerated water uptake and swelling of the seed due to increased seed coat permeability through cell wall loosening. Indeed, we found an increase in testa and/or mucilage permeability to tetrazolium in the presence of germination-accelerating concentrations of PME (Fig. 8). That this was a direct effect of the PME on the cell wall was demonstrated by a further increase in permeability when PG was also added. Treatment of *L. sativum* seeds with the allelochemical myrigalone A increases the coat permeability (Voegele et al., 2012). In Arabidopsis, mutants with an increased testa permeability (*transparent testa* mutants) germinate faster than the wild type (Debeaujon et al., 2000). Moreover, methanol, which is released by PME action, is known to be a hydroxyl radical scavenger. Hydroxyl radicals have been previously shown to promote cell wall loosening associated with ER during *L. sativum* seed germination (Müller et al., 2009). Hence, radical mediated loosening of the CAP may be interfered by the methanol

produced through high PME activity, as would be expected from exposure to high concentrations of PME.

Altogether, on the basis of our findings we conclude that *L. sativum* seed germination entails tightly regulated changes in the degree of pectin methylesterification through seed-compartment specific differential expression of PMEs and PMEIs.

Materials and Methods

Plant material and germination kinetics

For all experiments after-ripened seeds of *Lepidium sativum* L. FR14 ('Keimsprossen', Juliwa, Heidelberg, Germany) were used (Graeber et al., 2010). Seeds were incubated in Petri dishes with two layers of filter paper containing 6 ml of distilled and autoclaved water, sealed with parafilm and placed in a climate chamber with continuous light (ca. 100 µmol $s^{-1}m^{-2}$) at 24°C for the microarrays and at 18°C for the PME experiments. TR and ER were scored at the indicated times. Where indicated, orange peel PME (P5400, Sigma), (+)*cis-trans*-abscisic acid (ABA, Duchefa) or 1-aminocyclopropane-1-carboxylic acid (ACC, Sigma) was added in the indicated concentration.

RNA extraction and microarrays

L. sativum seed compartments (100 RADs, 100 CAPs, 200 NMEs, or 50 COTs) were homogenized in liquid nitrogen with a Precellys homogenisator for two cycles at 6100 rpm, thawed in 1 ml CTAB-buffer (2% [w/v] hexadecyl trimethyl-ammonium bromide (CTAB); 2% [w/v] polyvinylpyrrolidone PVP (MW=40000/K30); 100 mM Tris-HCl, pH 8.0; 25 mM EDTA, pH 8.0; 2 M NaCl; 2% [v/v] ß-mercaptoethanol) homogenized again and then incubated at 65°C for 15 min. After two extraction steps with 1 ml chloroform:isoamylalcohol (24:1 [v/v]) the volume of the hydrophilic phase was determined and ¼ of that volume 10 M LiCl was added. The RNA was precipitated at 4°C overnight. After centrifugation at 13000 rpm and 4°C, the pellet was resuspended in 600 µl SSTE-buffer (1 M NaCl; 0.5% [w/v]sodium dodecyl sulfate (SDS); 10 mM Tris-HCl, pH 8.0; 1 mM EDTA) and two more chloroform extractions were performed in PhaseLock vials. The RNA was precipitated with Na-Acetate/Ethanol at -20°C, the pellet washed with Ethanol, air-dried and resuspended in RNAse-free water. An RNeasy column clean-up was performed according to the manufacturer's instructions including the optional DNAse. Quality of the resulting RNA was assessed via nanodrop measurement, analytical gel electrophoresis and by integrity measurement on a bioanalyzer with a nanochip. RNAs were concentrated to 100 ng/µl and shipped on dry ice to ServiceXS (Leiden, NL), who performed the aRNA synthesis and hybridisations to the GeneChip Arabidopsis ATH1 Genome Array (Affymetrix, UK).

Probe Masking and Normalisation

Masking determines how many probes of each probe set are retained in the analysis. The commonly used method for cross-species masking is to perform experiments hybridising genomic DNA instead of RNA to the microarray, then masking probes whose DNA spot

intensity is below an arbitrary cutoff (Hammond et al., 2005). This method assumes that any probe which shows a low binding signal in the DNA hybridisation has no orthologous transcript of sufficient sequence similarity expressed in the species of interest, without taking into account that different probes have differing binding affinities. Instead, we performed an ANOVA on each probe individually to determine whether it is receiving signal or noise across conditions, allowing us to remove probes with no signal prior to normalisation. In support that performing this ANOVA did not introduced an undesirable bias, most of the reference genes identified from Arabidopsis and *L. sativum* seed transcriptomes (Dekkers et al., 2012; Graeber et al., 2011) have been kept in our masking process. To allocate the probes to probesets before masking, the Arabidopsis custom chip definition file (CDF) from the CustomCDF project (Ath1121501_At_TAIRG.cdf v14.0.0; Dai et al., 2005) was used. This CDF maps the individual probes to their genes in Arabidopsis, using recent sequencing information from The Arabidopsis Information Repository (TAIR, Lamesch et al., 2012); this eliminates the many-many relationship that exists in the original CDF. The probe-level spot intensities for all 107 chips, using the customCDF, were read into a matrix, which were then normalised to have equal medians across each chip; this helps correct for the fact that the overall intensity of the chips vary prior to attempting to determine whether each probe represents signal. For each probe a one-way Analysis of Variance (ANOVA) was used to test whether the mean expression across all conditions was the same, generating a p-value for each probe. A False Discovery Rate (FDR) was then applied to these p-values, with threshold 0.01, to give a list of probes which show significant differences across the conditions. The probes which failed this test were removed from consideration, as were any probesets with fewer than three probes remaining. In support that this ANOVA masking did not introduced an undesirable bias, of the 24 reference genes identified using Arabidopsis seed transcriptomes (Dekkers et al., 2012), all but one have been kept in our masking process. Further to this, of the 15 reference gene candidates identified using the *L. sativum* seed-compartment-specific CATMA microarrays (Graeber et al., 2011), one is not on the ATH1 microarrays and nine were kept (Supplemental Fig. S7). These nine reference gene candidates .include the three most stable reference genes for which the geometric mean was used for normalising our qRT-PCR analysis; these were validated as being stable in the RNA samples used in this work. The chips were then background corrected and normalised using Robust Multi-array Averaging (RMA) (Irizarry et al., 2003) with the CDF resulting from the above masking method. The microarray data including the normalised intensity values for each microarray of our *L. sativum* work were deposited in The National Center for Biotechnology Information's Gene Expression Omnibus with accession number GSE55702. Using the masking method presented here, with a False Discovery Rate of 0.01, 36.6% of

probes and 65.1% of probesets were retained, leading to 5793 genes identified as being differentially expressed between 1 hour after sowing and 16 hours after sowing in the CAP, and 6098 genes in the RAD. Conversely, using the method of (Hammond et al., 2005) the maximal number of differentially expressed genes was 1712 at a cutoff of 100. Thus our method retained a much larger number of differentially expressed genes that could then be used for further analysis.

Immunofluorescence microscopy

Preparation of plant materials and subsequent immunofluorescence microscopy with antibodies specific for specific cell-wall epitopes was conducted as described (Lee et al., 2012).

PME activity assay

Activity assays were performed as described (Downie et al., 1998) using esterified pectin from citrus fruit (P9561, Sigma) with >85% esterification with the following modifications: we used 4% (w/v) agarose, the incubation took place at 32°C and after ruthenium red staining an additional wash-step was carried out overnight. For protein extraction 100 RADs or 150 CAPs were ground in liquid nitrogen, and 200 µl extraction buffer (40 mM sodium acetate, pH 5.2) were added. The samples were incubated on a shaker at 4°C for 10 min and then centrifuged at 10000 rpm for 5 min at 4°C. For radicles and caps, 10 µl or 20 µl, respectively, of the supernatant were loaded directly into the wells of the agarose plate. For each time or treatment 3 biological replicates were used. To normalize enzyme activities, protein concentration in the extracts was determined using the Bio-Rad Protein Assay Solution. A standard curve for pectin methylesterase activity was carried out with commercial pectinesterase from orange peel (P5400, Sigma). Stained zones on the agarose plates were analyzed with ImageJ software and enzyme activity was calculated based on the standard curve (Supplemental Fig. S8).

Mathematical model of PME activity in seed compartments

A model was developed to describe the action of PME and PMEIs in altering methylesterified homogalacturonan (*MeHG*) into demethylesterified homogalacturonan (*dHG*). The two groups of PMEs (*G1*, *G2* respectively) and the PMEIs (*PMEI*) may form irreversible complexes (*PMEI:G1*, *PMEI:G2*), as well as the self-inactivation of group 2 PMEs to form an inactive version (*iG2*). The PME demethylesterification rates of group *i* PMEs is denoted α_i, the binding rates of the PMEI proteins with group *i* PMEs are denoted ζ_i. Group 2 PME molecules may inactivate themselves, in a unimolecular way, with binding rate ζ_3, whereas

653 the binding between PMEs and PMEIs are obviously bimolecular as reflected in the nonlinear
654 terms in equations 1-8. Transcript accumulation as measured from the microarrays for the
655 two groups of PMEs and the PMEIs were used as a proxy for protein accumulation, with $\beta_p(t)$
656 being the production of the mRNA corresponding to protein *p*, and *C* is a standardising
657 constant, to describe the relationship between protein and mRNA. To determine the values
658 of the constants, the results from the model were fitted to the *L. sativum* PME enzyme
659 activity data for the RAD and CAP shown in Fig. 5A, using Matlab's genetic algorithm. The
660 resulting PME activity predicted by the model after fitting is shown in Fig. 6D. The resulting
661 fitted parameters are shown in Supplemental Table S3.
662
663 **Testa permeability assay using tetrazolium**
664 Entire *L. sativum* seeds were incubated for 9 h in continuous light at 18 °C with tetrazolium
665 staining solution (Graeber *et al.*, 2010; Voegele et al., 2012) containing the indicated
666 concentrations of PME (P5400, Sigma) or PG (17389, Sigma). The embryos were
667 subsequently extracted, classified according to their staining intensity and patterns, and
668 photographed.
669
670 **In situ *mRNA* hybridization**
671 For *LesaPME11580* a forward primer with a additional *Bam*HI restriction site
672 (ATGGATCCAGCAGTGACTGCAGCACCG) and a reverse primer with an *Eco*RI site
673 (ATGAATTCCGTGTGAGTGTAGAGCGTGT) were used to amplify a probe of 353 bp length
674 from reverse transcribed RNA isolated from *L. sativum* seeds. The probe spanned the
675 pectinesterase domain. After digestion with *Bam*H1 and *Eco*R1, the product was cloned into
676 the pBluescript II KS+ vector. For the sense probe, the plasmid was linearized with *Xba*1 and
677 transcribed with T3 polymerase (Promega), while for the antisense probe *Hind*III was used
678 for linearization and T7 polymerase (Promega) for transcription with the digoxigenin-labelling
679 kit (Roche) was used. Finally, the *in situ* hybridization was performed as described previously
680 using 400 ng probe per slide (Mayer et al., 1998).
681
682 **Sequence alignments, molecular phylogenetic analysis and eNorthern analysis**
683 For all sequence and phylogenetic analyses, the bioinformatic software Geneious 5.0.4.
684 (Biomatters, Auckland, New Zealand) was used. Multiple sequence alignment on the basis of
685 amino acid sequences of PMEs and PMEIs from different species was performed using the
686 Muscle algorithm with default settings. For the phylogenetic tree, two different algorithms,
687 Mafft and Muscle, were used and also two methods for the tree construction, maximum-
688 likelihood (PHYML software) and Bayesian inference (MrBayes software). The eNorthern tool

689 based on global transcriptome analysis of Arabdiopsis at www.bar.utoronto.ca (Winter et al.,
690 2007) was used for visualisation of transcript expression patterns of Arabidopsis PMEs and
691 PMEI.
692
693 **Analyses of the relative transcript abundance by quantitative real-time RT-PCR (qRT-**
694 **PCR)**
695 The cDNA synthesis and the qRT-PCR was performed as previously described using
696 LesaG17210, LesaG20000 and LesaG04320 as reference genes (Graeber et al., 2011).
697 Analysis of all raw data, calculation of the efficiency (E) and CT values were carried out with
698 the PCR miner software. The relative transcript abundance for every well was calculated as
699 (1+E)^(-CT) and normalized against the geometric mean of the reference genes. The mean
700 value of four biological replicates ±SE are shown. All primers were designed with the
701 Geneious 5.0.4. software. Cloned cDNAs were sequenced and have been deposited as
702 ESTs or full length sequences to GenBank. Accession numbers and primer sequences are
703 listed in Supplemental Table S4.
704
705 **LITERATURE CITED**
706
707 **Bewley JD** (1997) Seed germination and dormancy. Plant Cell **9**: 1055–1066
708 **Braybrook SA, Hofte H, Peaucelle A** (2012) Probing the mechanical contributions of the
709 pectin matrix: insights for cell growth. Plant Signal Behav **7**: 1037–1041
710 **Braybrook SA, Peaucelle A** (2013) Mechano-chemical aspects of organ formation in
711 *Arabidopsis thaliana*: the relationship between auxin and pectin. PLoS One **8**: e57813
712 **Cosgrove DJ, Jarvis MC** (2012) Comparative structure and biomechanics of plant primary
713 and secondary cell walls. Front Plant Sci **3**: 204
714 **Dai M, Wang P, Boyd AD, Kostov G, Athey B, Jones EG, Bunney WE, Myers RM, Speed**
715 **TP, Akil H, et al** (2005) Evolving gene/transcript definitions significantly alter the
716 interpretation of GeneChip data. Nucleic Acids Res **33**: e175
717 **Debeaujon I, Léon-Kloosterziel KM, Koornneef M** (2000) Influence of the testa on seed
718 dormancy, germination, and longevity in Arabidopsis. Plant Physiol **122**: 403–414
719 **Dekkers BJW, Pearce S, van Bolderen-Veldkamp RP, Marshall A, Widera P, Gilbert J,**
720 **Drost H-G, Bassel GW, Müller K, King JR, et al** (2013) Transcriptional dynamics of two
721 seed compartments with opposing roles in Arabidopsis seed germination. Plant Physiol **163**:
722 205–215

Dekkers BJ, Willems L, Bassel GW, van Bolderen-Veldkamp RP, Ligterink W, Hilhorst HW, Bentsink L (2012) Identification of reference genes for RT-qPCR expression analysis in Arabidopsis and tomato seeds. Plant Cell Physiol **53** 28-37

Downie B, Dirk LM, Hadfield KA, Wilkins TA, Bennett AB, Bradford KJ (1998) A gel diffusion assay for quantification of pectin methylesterase activity. Anal Biochem **264**: 149–157

Eckardt NA (2005) VANGUARD1 - At the forefront of pollen tube growth. Plant Cell **17**: 327–329

Endo A, Tatematsu K, Hanada K, Duermeyer L, Okamoto M, Yonekura-Sakakibara K, Saito K, Toyoda T, Kawakami N, Kamiya Y, et al (2012) Tissue-specific transcriptome analysis reveals cell wall metabolism, flavonol biosynthesis and defense responses are activated in the endosperm of germinating *Arabidopsis thaliana* seeds. Plant Cell Physiol **53**: 16–27

Giovane A, Servillo L, Balestrieri C, Raiola A, D'Avino R, Tamburrini M, Ciardiello MA, Camardella L (2004) Pectin methylesterase inhibitor. Biochim Biophys Acta **1696**: 245–252

Gonzalez-Carranza ZH, Elliott KA, Roberts JA (2007) Expression of polygalacturonases and evidence to support their role during cell separation processes in *Arabidopsis thaliana*. J Exptl Bot **58:** 3719-3730

Graeber K, Linkies A, Müller K, Wunchova A, Rott A, Leubner-Metzger G (2010) Cross-species approaches to seed dormancy and germination: conservation and biodiversity of ABA-regulated mechanisms and the Brassicaceae *DOG1* genes. Plant Mol Biol **73**: 67–87

Graeber K, Linkies A, Steinbrecher T, Mummenhoff K, Tarkowská D, Turečková V, Ignatz M, Sperber K, Voegele A, de Jong H, Urbanová T, Strnad M, Leubner-Metzger G (2014) DELAY OF GERMINATION 1 mediates a conserved coat dormancy mechanism for the temperature- and gibberellin-dependent control of seed germination. Proceedings of the National Academy of Sciences of the United States of America **111**: E3571–E3580

Graeber K, Linkies A, Wood ATA, Leubner-Metzger G (2011) A guideline to family-wide comparative state-of-the-art quantitative RT-PCR analysis exemplified with a Brassicaceae cross-species seed germination case study. Plant Cell **23**: 2045–2063

Hammond JP, Bowen HC, White PJ, Mills V, Pyke KA, Baker AJM, Whiting SN, May ST, Broadley MR (2006) A comparison of the *Thlaspi caerulescens* and *Thlaspi arvense* shoot transcriptomes. New Phytol **170**: 239–260

Hammond JP, Broadley MR, Craigon DJ, Higgins J, Emmerson ZF, Townsend HJ, White PJ, May ST (2005) Using genomic DNA-based probe-selection to improve the sensitivity of high-density oligonucleotide arrays when applied to heterologous species. Plant Methods **1**: 10

Hyodo H, Terao A, Furukawa J, Sakamoto N, Yurimoto H, Satoh S, Iwai H (2013) Tissue specific localization of pectin-Ca^{2+} cross-linkages and pectin methyl-esterification during fruit ripening in tomato (*Solanum lycopersicum*). PLoS One **8**: e78949

Iglesias-Fernandez R, Rodriguez-Gacio MdC, Barrero-Sicilia C, Carbonero P, Matilla A (2011) Three endo-beta-mannanase genes expressed in the micropylar endosperm and in the radicle influence germination of *Arabidopsis thaliana* seeds. Planta **233:** 25-36

Irizarry RA, Hobbs B, Collin F, Beazer-Barclay YD, Antonellis KJ, Scherf U, Speed TP (2003) Exploration, normalization, and summaries of high density oligonucleotide array probe level data. Biostatistics **4**: 249–264

Kucera B, Cohn MA, Leubner-Metzger G (2005) Plant hormone interactions during seed dormancy release and germination. Seed Sci Res **15**: 281–307

Lamesch P, Berardini TZ, Li D, Swarbreck D, Wilks C, Sasidharan R, Muller R, Dreher K, Alexander DL, Garcia-Hernandez M, et al (2012) The Arabidopsis Information Resource (TAIR): improved gene annotation and new tools. Nucleic Acids Res **40**: D1202–10

Lee KJD, Dekkers BJW, Steinbrecher T, Walsh CT, Bacic A, Bentsink L, Leubner-Metzger G, Knox JP (2012) Distinct cell wall architectures in seed endosperms in representatives of the Brassicaceae and Solanaceae. Plant Physiol **160**: 1551–1566

Leubner-Metzger G (2001) Brassinosteroids and gibberellins promote tobacco seed germination by distinct pathways. Planta **213:** 758-763

Linkies A, Leubner-Metzger G (2012) Beyond gibberellins and abscisic acid: how ethylene and jasmonates control seed germination. Plant Cell Reports **31:** 253-270

Linkies A, Müller K, Morris K, Turecková V, Wenk M, Cadman CSC, Corbineau F, Strnad M, Lynn JR, Finch-Savage WE, et al (2009) Ethylene interacts with abscisic acid to regulate endosperm rupture during germination: a comparative approach using *Lepidium sativum* and *Arabidopsis thaliana*. Plant Cell **21**: 3803–3822

Liu P-P, Koizuka N, Martin RC, Nonogaki H (2005) The BME3 (Blue Micropylar End 3) GATA zinc finger transcription factor is a positive regulator of Arabidopsis seed germination. Plant J **44**: 960–71

Manz B, Müller K, Kucera B, Volke F, Leubner-Metzger G (2005) Water uptake and distribution in germinating tobacco seeds investigated *in vivo* by nuclear magnetic resonance imaging. Plant Physiol **138**: 1538-1551

Markovic O, Janecek S (2004) Pectin methylesterases: sequence-structural features and phylogenetic relationships. Carbohydr Res **339**: 2281–2295

Martínez-Andújar C, Pluskota WE, Bassel GW, Asahina M, Pupel P, Nguyen TT, Takeda-Kamiya N, Toubiana D, Bai B, Górecki RJ, et al (2012) Mechanisms of hormonal regulation of endosperm cap-specific gene expression in tomato seeds. Plant J **71**: 575–86

Mayer KF, Schoof H, Haecker A, Lenhard M, Jürgens G, Laux T (1998) Role of WUSCHEL in regulating stem cell fate in the Arabidopsis shoot meristem. *Cell* **95**: 805-815

Mohnen D (2008) Pectin structure and biosynthesis. Curr Opin Plant Biol **11**: 266–77

Morris K, Linkies A, Müller K, Oracz K, Wang X, Lynn JR, Leubner-Metzger G, Finch-Savage WE (2011) Regulation of seed germination in the close Arabidopsis relative *Lepidium sativum*: a global tissue-specific transcript analysis. Plant Physiol **155**: 1851–1870

Müller K, Levesque-Tremblay G, Bartels S, Weitbrecht K, Wormit A, Usadel B, Haughn G, Kermode AR (2013) Demethylesterification of cell wall pectins in Arabidopsis plays a role in seed germination. Plant Physiol **161**: 305–316

Müller K, Linkies A, Vreeburg RAM, Fry SC, Krieger-Liszkay A, Leubner-Metzger G (2009) *In vivo* cell wall loosening by hydroxyl radicals during cress seed germination and elongation growth. Plant Physiol **150**: 1855–1865

Müller K, Tintelnot S, Leubner-Metzger G (2006) Endosperm-limited Brassicaceae seed germination: abscisic acid inhibits embryo-induced endosperm weakening of *Lepidium sativum* (cress) and endosperm rupture of cress and *Arabidopsis thaliana*. Plant Cell Physiol **47**: 864–877

Nonogaki H, Gee OH, Bradford KJ (2000) A germination-specific endo-beta-mannanase gene is expressed in the micropylar endosperm cap of tomato seeds. Plant Physiol **123**: 1235–1246

Peaucelle A, Louvet R, Johansen JN, Salsac F, Morin H, Fournet F, Belcram K, Gillet F, Höfte H, Laufs P, et al (2011) The transcription factor BELLRINGER modulates phyllotaxis by regulating the expression of a pectin methylesterase in Arabidopsis. Development **138**: 4733–41

Pelletier S, Van Orden J, Wolf S, Vissenberg K, Delacourt J, Ndong YA, Pelloux J, Bischoff V, Urbain A, Mouille G, et al (2010) A role for pectin de-methylesterification in a developmentally regulated growth acceleration in dark-grown Arabidopsis hypocotyls. New Phytol **188**: 726–39

Pelloux J, Rustérucci C, Mellerowicz EJ (2007) New insights into pectin methylesterase structure and function. Trends Plant Sci **12**: 267–77

Ren C, Kermode AR (2000) An increase in pectin methyl esterase activity accompanies dormancy breakage and germination of yellow cedar seeds. Plant Physiol **124**: 231–42

Saez-Aguayo S, Ralet MC, Berger A, Botran L, Ropartz D, Marion-Poll A, North HM (2013) PECTIN METHYLESTERASE INHIBITOR6 promotes Arabidopsis mucilage release by limiting methylesterification of homogalacturonan in seed coat epidermal cells. Plant Cell **25:** 308-323

Schopfer P (2006) Biomechanics of plant growth. Am J Bot **93**: 1415–25

Slotte T, Holm K, McIntyre LM, Lagercrantz U, Lascoux M (2007) Differential expression of genes important for adaptation in *Capsella bursa-pastoris* (Brassicaceae). Plant Physiol **145**: 160–73

Steber CM (2001) A role for brassinosteroids in germination in Arabidopsis. Plant Physiol **125**: 763–769

Tan L, Eberhard S, Pattathil S, Warder C, Glushka J, Yuan C, Hao Z, Zhu X, Avci U, Miller JS, et al (2013) An Arabidopsis cell wall proteoglycan consists of pectin and arabinoxylan covalently linked to an arabinogalactan protein. Plant Cell **25**: 270–287

Thompson DS (2005) How do cell walls regulate plant growth? J Exptl Bot **56**: 2275–85

Voegele A, Linkies A, Müller K, Leubner-Metzger G (2011) Members of the gibberellin receptor gene family *GID1* (*GIBBERELLIN INSENSITIVE DWARF1*) play distinct roles during *Lepidium sativum* and *Arabidopsis thaliana* seed germination. J Exptl Bot **62:** 5131–5147

Voegele A, Graeber K, Oracz K, Tarkowská D, Jacquemoud D, Turečková V, Urbanová T, Strnad M, Leubner-Metzger G (2012) Embryo growth, testa permeability, and endosperm weakening are major targets for the environmentally regulated inhibition of *Lepidium sativum* seed germination by myrigalone A. J Exptl Bot **63**: 5337–5350

Wakabayashi K, Chun J-P, Huber DJ (2000) Extensive solubilization and depolymerization of cell wall polysaccharides during avocado (*Persea americana*) ripening involves concerted action of polygalacturonase and pectinmethylesterase. Physiol Plant **108**: 345–352

Wakabayashi K, Hoson T, Huber DJ (2003) Methyl de-esterification as a major factor regulating the extent of pectin depolymerization during fruit ripening: a comparison of the action of avocado (*Persea americana*) and tomato (*Lycopersicon esculentum*) polygalacturonases. J Plant Physiol **160**: 667–673

Wang M, Yuan D, Gao W, Li Y, Tan J, Zhang X (2013) A comparative genome analysis of PME and PMEI families reveals the evolution of pectin metabolism in plant cell walls. PLoS One **8**: e72082

Willats WGT, McCartney L, Mackie W, Knox JP (2001) Pectin: cell biology and prospects for functional analysis. Plant Mol Biol **47**: 9–27

Winter D, Vinegar B, Nahal H, Ammar R, Wilson GV, Provart NJ (2007) An "electronic fluorescent pictograph" browser for exploring and analyzing large-scale biological data sets. PLoS ONE **2:** e718

Wolf S, Mouille G, Pelloux J (2009a) Homogalacturonan methyl-esterification and plant development. Mol Plant **2**: 851–60

Wolf S, Mravec J, Greiner S, Mouille G, Höfte H (2012) Plant cell wall homeostasis is mediated by brassinosteroid feedback signaling. Curr Biol **22**: 1732–1737

Wolf S, Rausch T, Greiner S (2009b) The N-terminal pro region mediates retention of unprocessed type-I PME in the Golgi apparatus. Plant J **58**: 361–375

Yang XY, Zeng ZH, Yan JY, Fan W, Bian HW, Zhu MY, Yang JL, Zheng SJ (2013) Association of specific pectin methylesterases with Al-induced root elongation inhibition in rice. Physiol Plant **148**: 502–511

Yoshida S, Barbier de Reuille P, Lane B, Bassel GW, Prusinkiewicz P, Smith RS, Weijers D (2014) Genetic control of plant development by overriding a geometric division rule. Developmental Cell **29:** 75-87

Figure legends:

Figure 1. Spatio-temporal transcriptome analysis of *Lepidium sativum* FR14 seed compartments during germination. **(A)** The kinetics of *L. sativum* testa rupture (TR) and endosperm rupture (ER) at 24ºC in continuous light. Arrows indicate sampling times points for RNA extraction at which the seeds were dissected into CAP, RAD, COT and NME, as indicated. Note that at 0h (dry seed stage) CAP plus RAD as well as NME+COT were sampled together. Mean values ±SE of N=4 plates each with 100 seeds are presented for TR and ER. **(B)** *L. sativum* seed compartments (CAP, RAD, COT and NME) at different stages during germination as related to the TR and ER kinetics. **(C)** Principal Components Analysis (PCA) of the *L. sativum* microarray results with four biological RNA replicates for each time point. *Eigenvector 1* separates transcriptomes in time while *eigenvector 2* separates the seed compartments. For abbreviations of compartments and seed states see (A) and (B).

Figure 2. Immunolocalisation of the LM19 HG and JIM7 Me-HG pectin cell wall epitopes in longitudinal sections of germinating *Lepidium sativum* seeds 3 h after imbibition (3 h), at testa rupture (TR) and at endosperm rupture (ER). Immunodetection with LM19 indicates the ubiquitous distribution of HG in all cell walls of the embryo, endosperm (E), at the testa surface (T) and in mucilage (M). By contrast, immunodetection with JIM7 indicates the occurrence of Me-HG is restricted to the mucilage and testa surface with reduced levels detectable in the radicle at 3 h. Comparative high magnification micrographs of endosperm tissue at 3 h indicates absence of the JIM7 epitope and its appearance in endosperm cell walls by TR suggesting deposition of newly synthesized HG. Arrowheads with E and T indicate ruptured endosperm and testa respectively.

Figure 3. Phylogeny of *Arabidopsis thaliana* PMEs and PMEIs and transcript expression in germinating seeds. Phylogenetic analysis of the predicted full-length amino acid sequences of 136 PMEs and PMEIs (Supplemental Data Set S4) from reveal three distinct phylogenetic groups: PME group 1 (yellow) with specific PME domain, PME group 2 (rose) with PME domain and inhibitory domain and PMEI (blue) with just the inhibitory domain. We used the MUSCLE algorithm for the amino acid multiple sequence alignment, and a maximum-likelihood tree was constructed using the PYHML-. A similar tree topology, i.e. the same major clusters and subclusters, were also obtained when a different alignment algorithm was used (MAFFT). We used several PMEs of *Paenibacillus mucilaginosus KNP414* as outgroup. Note that in our phylogenetic analysis three sequences of PME enzymes without PMEI domains are localized within the PME group 2 (highlighted with white background) due to the

913 high similarity of their PME domains to the PME domain of the group 2. One of these three
914 PMEs, At3g10720, generates two different RNAs by alternative splicing. If both RNAs are
915 translated, they would produce a group 1 PME (At3g10720.1) and a group 2 PME
916 (At3g10720.2) protein, respectively. *Columns at the right next to the AGI numbers:* Results
917 from eNorthern analysis for Arabidopsis seed cold stratification (1), imbibition (2) and ABA
918 treatment (3); red color indicates an up-regulation, blue down-regulation and white no
919 regulation in entire seeds. Grey colored genes are not present in the datasets used. The
920 transcriptome analysis available via the seed-specific eFP-browser at www.bar.utoronto.ca
921 on which this analysis was based with non-dormant, after-ripened wild-type seeds. Structural
922 motifs according to Pelloux et al. (2007): SP, signal peptide; TM, transmembrane domain;
923 PM, processing motif.
924
925 **Figure 4.** Seed compartment specific expression patterns of PMEs and PMEIs in *Lepidium*
926 *sativum* and Arabidopsis. *Top panels:* Heat maps showing expression patterns of PME and
927 PMEI transcripts in our microarrays of the *L. sativum* CAP (micropylar endosperm; *left*
928 *panel*), compared to the expression of the putative Arabidopsis orthologue in the Arabidopsis
929 MCE (CAP plus chalazal endosperm; *right panel*). *Bottom panels:* showing expression
930 patterns of PME and PMEI transcripts in our microarrays of the *L. sativum* RAD (*left panel*),
931 compared to the expression of the putative Arabidopsis orthologue in the Arabidopsis RAD
932 (*right panel*). The Arabidopsis results were extracted from the microarray database published
933 by Dekkers et al. (2013). Note that in contrast to *L. sativum* (Fig. 1B) the Arabidopsis "CAP
934 compartment" contains the chalazal endosperm in addition to the micropylar endosperm, and
935 the Arabidopsis "RAD compartment" contains upper hypocotyl in addition to the lower
936 hypocotyl (embryo growth zone) and radicle (Dekkers et al., 2013).
937
938 **Figure 5.** PME enzyme activity during the seed germination of *Lepidium sativum*. Seeds
939 were imbibed in **(A)** water (CON, control) or **(B)** 5 µM abscisic acid (ABA). The kinetics of *L.*
940 *sativum* testa rupture (TR) and endosperm rupture (ER) at 18ºC in continuous light. PME
941 enzyme activity was measured for protein extracts of CAP and RAD excised from imbibed
942 seeds at the times indicated. Mean values ±SE for four biological replicates with 100 seeds
943 each are presented.
944
945 **Figure 6.** Mathematical model of contributions of group 1 PMEs, group 2 PMEs, and PMEIs
946 to overall PME activity in RAD and CAP during *L. sativum* seed germination. **(A)** Network
947 Diagram, where α_i are the rates at which MeHG is de-methylesterified and ζ_i the rates at
948 which a PMEI domain binds with a PME domain. **(B)** Plots of the β functions: cumulative

949 transcript levels for each group, within the CAP and RAD of *L. sativum* during germination;
950 these levels are used as approximations of protein production. **(C)** Ordinary Differential
951 Equations (ODE) based on our network model and the law of mass action. **(D)** Predicted
952 PME activities when using the *L. sativum* PME model, and fitting to the *L. sativum* data (Fig.
953 5A) for PME enzyme activity within the CAP and the RAD. For a detailed description of the
954 modelling see Materials and Methods, and for the parameter values for the mathematical
955 model see Supplemental Table S3.
956
957 **Figure 7.** Spatial and temporal analysis of transcript abundances of novel *Lepidium sativum*
958 *(Lesa)* group 2 PMEs in germinating seeds (18ºC, continuous light) by quantitative RT-PCR.
959 **(A)** PME enzyme activities as determined in Figure 5; note that scales for CAP and RAD are
960 different; note further that only intact CAPs (and corresponding RADs) were used at both
961 time points. **(B-E)** Normalized transcript abundances of selected group 2 PMEs. Seeds were
962 imbibed without (CON, control) or with ABA (5 µM). Micropylar endosperm (CAP) and the
963 lower 1/3 of the radicle/hypocotyl axis (RAD) were excised from seeds; results for CAP (*left*)
964 and RAD (*right*) are displayed on identical scales. *Early germination:* seeds after TR, but
965 prior to ER (16 h). *Late germination:* seeds at $ER_{50\%}$, which was ca. 22 h for CON, ca. 65 h
966 for ABA. Only unruptured CAPs were sampled. *Lesa17210, Lesa04320* and *Lesa20000*
967 (Graeber et al. 2011) were used as references genes for the qRT-PCR normalization as
968 described in the methods. Mean values ± SE for four biological replicates. Statistical
969 significance of CAP and RAD results were analysed separately by one-way ANOVA with
970 Tukey's multiple comparison test performed using GraphPad Prism software (version 4.0,
971 GraphPad Software, San Diego California USA, www.graphpad.com). Mean values labelled
972 with distinct letters differ significantly from each other with a P value <0.05.
973
974 **Figure 8.** Treatment of *Lepidium sativum* seeds with low amounts of PME promotes testa
975 rupture and enhances testa permeability. **(A)** Treatment of imbibed seeds low amounts (0.2
976 U, i.e. 0.03 U/ml) of orange peel PME promoted but did not affect ER. This promotion of TR
977 was by low PME amounts was not affected by simultaneous treatment with ABA or ACC.
978 Note that in contrast to low amounts, relatively high amounts (ca. 20 U) of PME delayed TR
979 and ER (Supplemental Fig. S5). Seeds were imbibed at 18ºC in continuous light; mean
980 values ±SE of four biological replicates are shown. **(B)** Treatment of seeds with PME and
981 pectin degradation by polygalacturonase (PG) enhances testa permeability as determined
982 using the tetrazolium assay. Seeds were imbibed for 9h in tetrazolium salt assay solution
983 without (CON) or with 0.2 U PME or PME+PG added. Embryos were excised and classified
984 into five staining groups: pale (no staining, testa impermeable for tetrazolium salts), yellow

(low testa permeability), and three categories of red (from partly to almost fully red, see Supplemental Fig. S6). Relative numbers based on 50 embryos for each series are presented. For different subcategories of red-stained embryos see Supplemental Fig. S6. Red embryo staining is indicative for increased testa permeability.

Supplemental Data

The following materials are available in the online version of this article.

Supplemental Figure S1. Cluster analysis of the *L. sativum* differentially regulated transcriptome over time and seed compartments.

Supplemental Figure S2. Amino acid sequence alignment of *L. sativum* PMEs and PMEIs.

Supplemental Figure S3. Spatial and temporal qRT-PCR analysis of PME and PMEI transcript abundances in germinating *L. sativum* seeds.

Supplemental Figure S4. *In situ* mRNA hybridization detection of *L. sativum* PME group-2 *LesaPME11580* transcripts.

Supplemental Figure S5. The effect of exogenous treaments of *L. sativum* seeds with PME on testa and endosperm rupture.

Supplemental Figure S6. The effect of exogenous treaments of *L. sativum* seeds with PME and pectin degradation by polygalacturonase (PG) on testa permeability.

Supplemental Figure S7. PME enzyme activity assay method.

Supplemental Table S1. Overrepresentation analysis of GO terms for CAP genes differentially up-regulated during testa rupture.

Supplemental Table S2. Overrepresentation analysis of GO terms for RAD genes differentially up-regulated during testa rupture.

Supplemental Table S3. Parameter values for the mathematical model.

Supplemental Table S4. Gene bank accession numbers and primer sequences.

Supplemental Data Set S1. Normalized $\log_2$ expression values from individual microarrays for the *Lepidium sativum* seed compartments (13895 transcripts).

Supplemental Data Set S2. Normalized $\log_2$ expression mean values for the *Lepidium sativum* seed compartments (13895 transcripts).

Supplemental Data Set S3. Normalized $\log_2$ expression SD values for the *Lepidium sativum* seed compartments (13895 transcripts).

Supplemental Data Set S4. *Arabidopsis thaliana* group 1 and 2 PMEs and PMEIs.

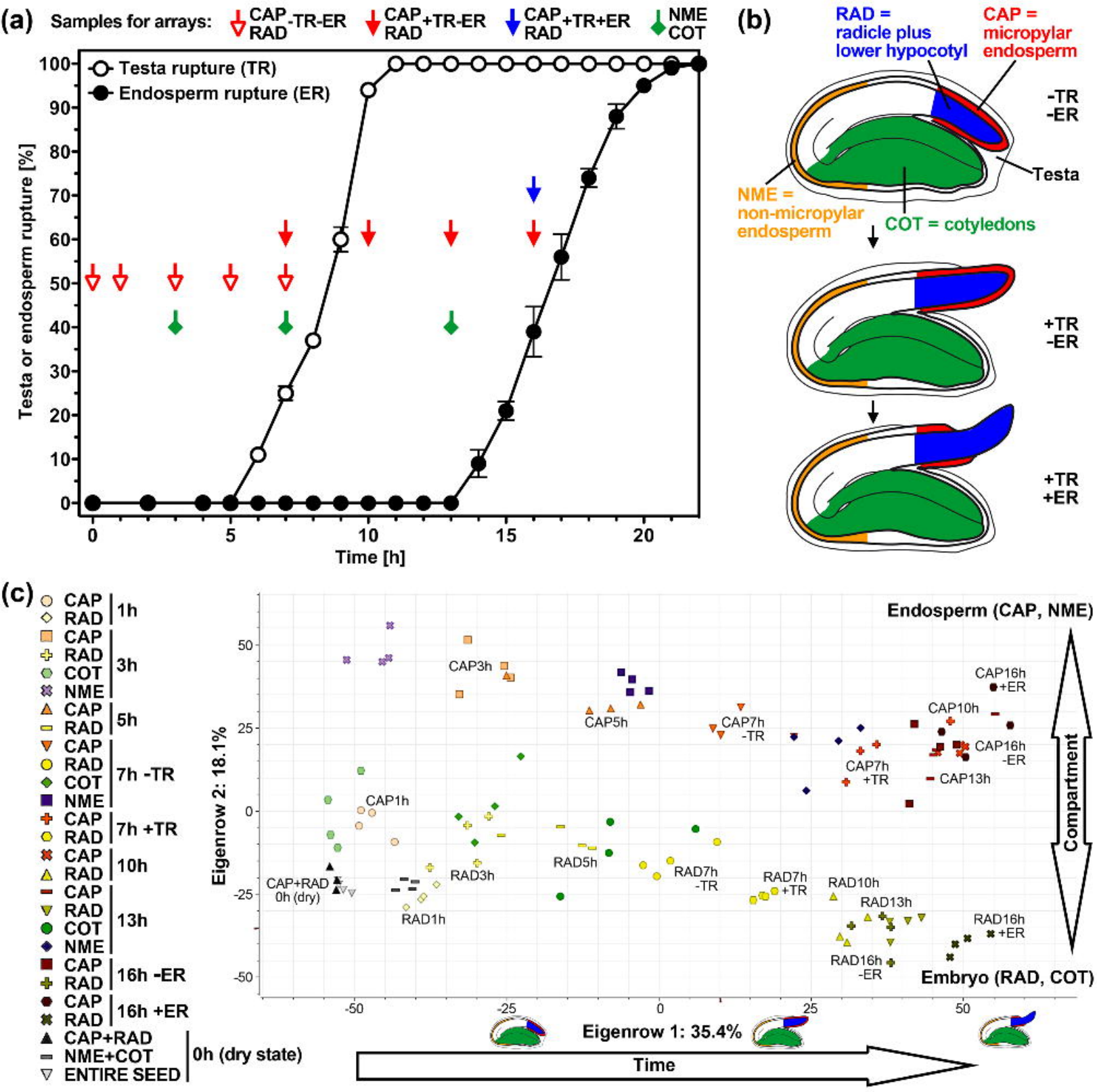

Figure 1. Spatio-temporal transcriptome analysis of Lepidium sativum FR14 seed compartments during germination. (A) The kinetics of L. sativum testa rupture (TR) and endosperm rupture (ER) at 24ºC in continuous light. Arrows indicate sampling times points for RNA extraction at which the seeds were dissected into CAP, RAD, COT and NME, as indicated. Note that at 0h (dry seed stage) CAP plus RAD as well as NME+COT were sampled together. Mean values ±SE of N=4 plates each with 100 seeds are presented for TR and ER. (B) L. sativum seed compartments (CAP, RAD, COT and NME) at different stages during germination as related to the TR and ER kinetics. (C) Principal Components Analysis (PCA) of the L. sativum microarray results with four biological RNA replicates for each time point. Eigenvector 1 separates transcriptomes in time while eigenvector 2 separates the seed compartments. For abbreviations of compartments and seed states see (A) and (B).

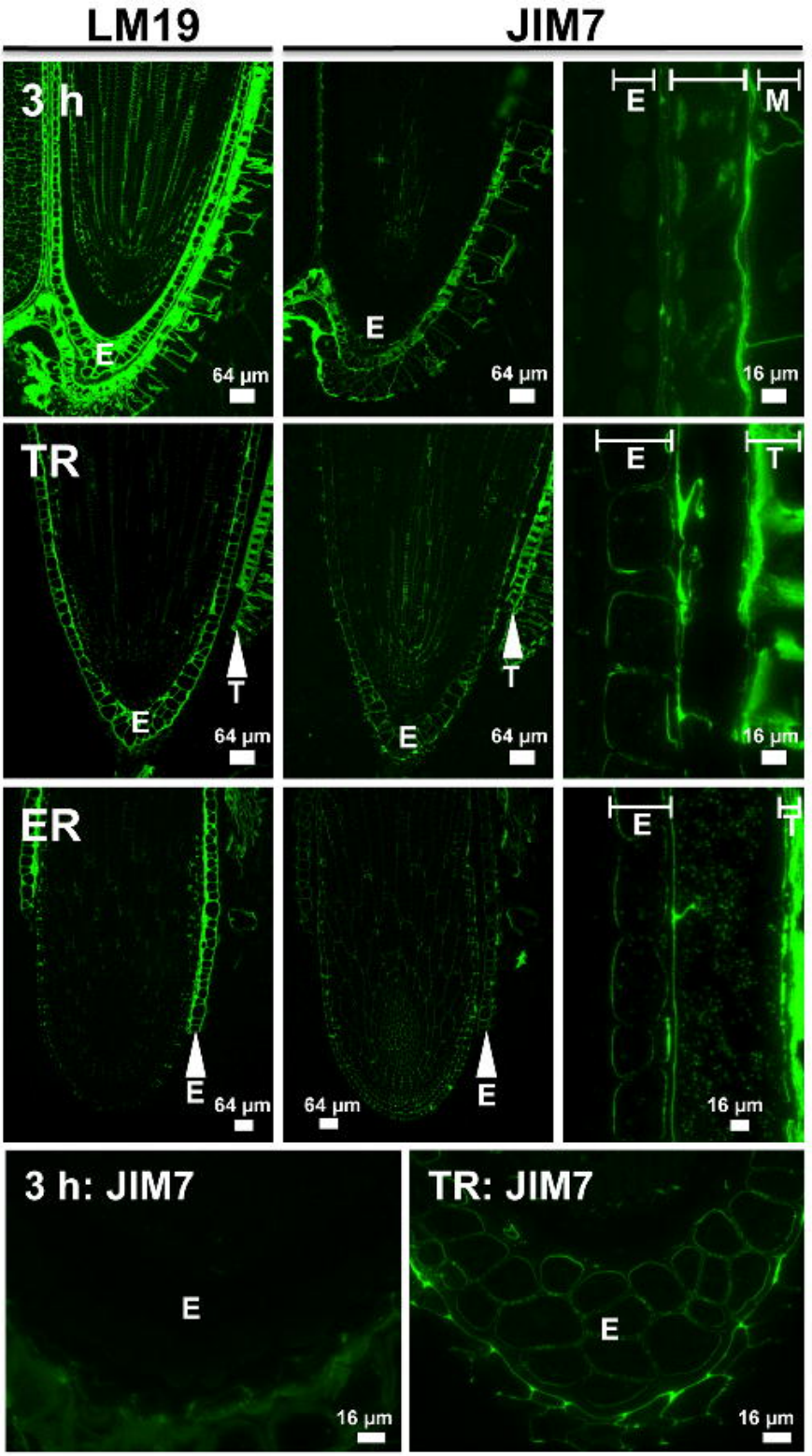

Figure 2. Immunolocalisation of the LM19 HG and JIM7 Me-HG pectin cell wall epitopes in longitudinal sections of germinating Lepidium sativum seeds 3 h after imbibition (3 h), at testa rupture (TR) and at endosperm rupture (ER). Immunodetection with LM19 indicates the ubiquitous distribution of HG in all cell walls of the embryo, endosperm (E), at the testa surface (T) and in mucilage (M). By contrast, immunodetection with JIM7 indicates the occurrence of Me-HG is restricted to the mucilage and testa surface with reduced levels detectable in the radicle at 3 h. Comparative high magnification micrographs of endosperm tissue at 3 h indicates absence of the JIM7 epitope and its appearance in endosperm cell walls by TR suggesting deposition of newly synthesized HG. Arrowheads with E and T indicate ruptured endosperm and testa respectively.

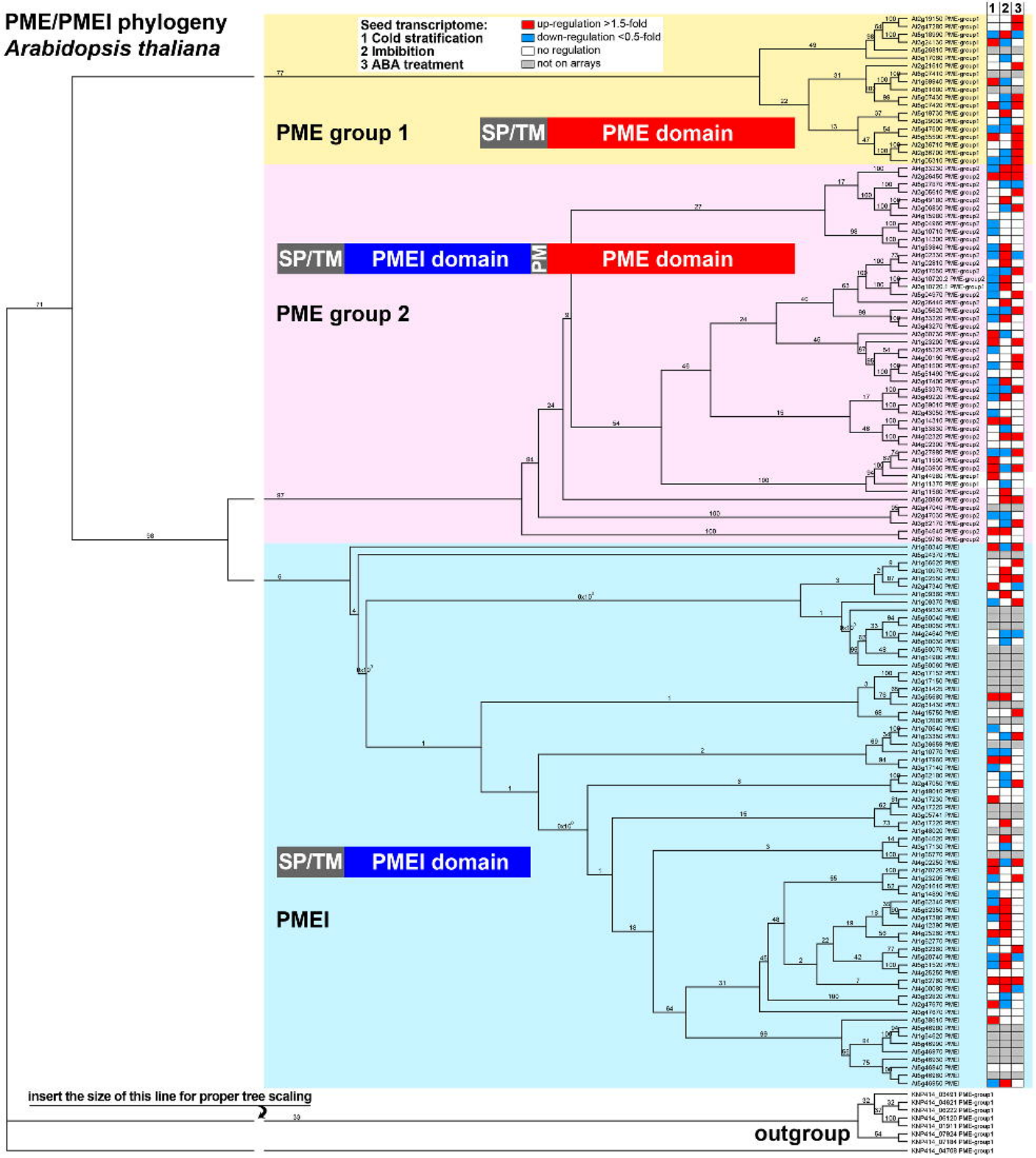

Figure 3. Phylogeny of Arabidopsis thaliana PMEs and PMEIs and transcript expression in germinating seeds. Phylogenetic analysis of the predicted full-length amino acid sequences of 136 PMEs and PMEIs from reveal three distinct phylogenetic groups: PME group 1 (yellow) with specific PME domain, PME group 2 (rose) with PME domain and inhibitory domain and PMEI (blue) with just the inhibitory domain. We used the MUSCLE algorithm for the amino acid multiple sequence alignment, and a maximum-likelihood tree was constructed using the PYHML-. A similar tree topology, i.e. the same major clusters and subclusters, were also obtained when a different alignment algorithm was used (MAFFT). We used several PMEs of Paenibacillus mucilaginosus KNP414 as outgroup. Columns at the right next to the AGI numbers: Results from eNorthern analysis for Arabidopsis seed cold stratification (1), imbibition (2) and ABA treatment (3); red color indicates an up-regulation, blue down-regulation and white no regulation in entire seeds. Grey colored genes are not present in the data-sets used. The transcriptome analysis available via the seed-specific eFP-browser at www.bar.utoronto.ca on which this analysis was based with non-dormant, after-ripened wild-type seeds. Structural motifs according to Pelloux et al. (2007): SP, signal peptide; TM, transmembrane domain; PM, processing motif.

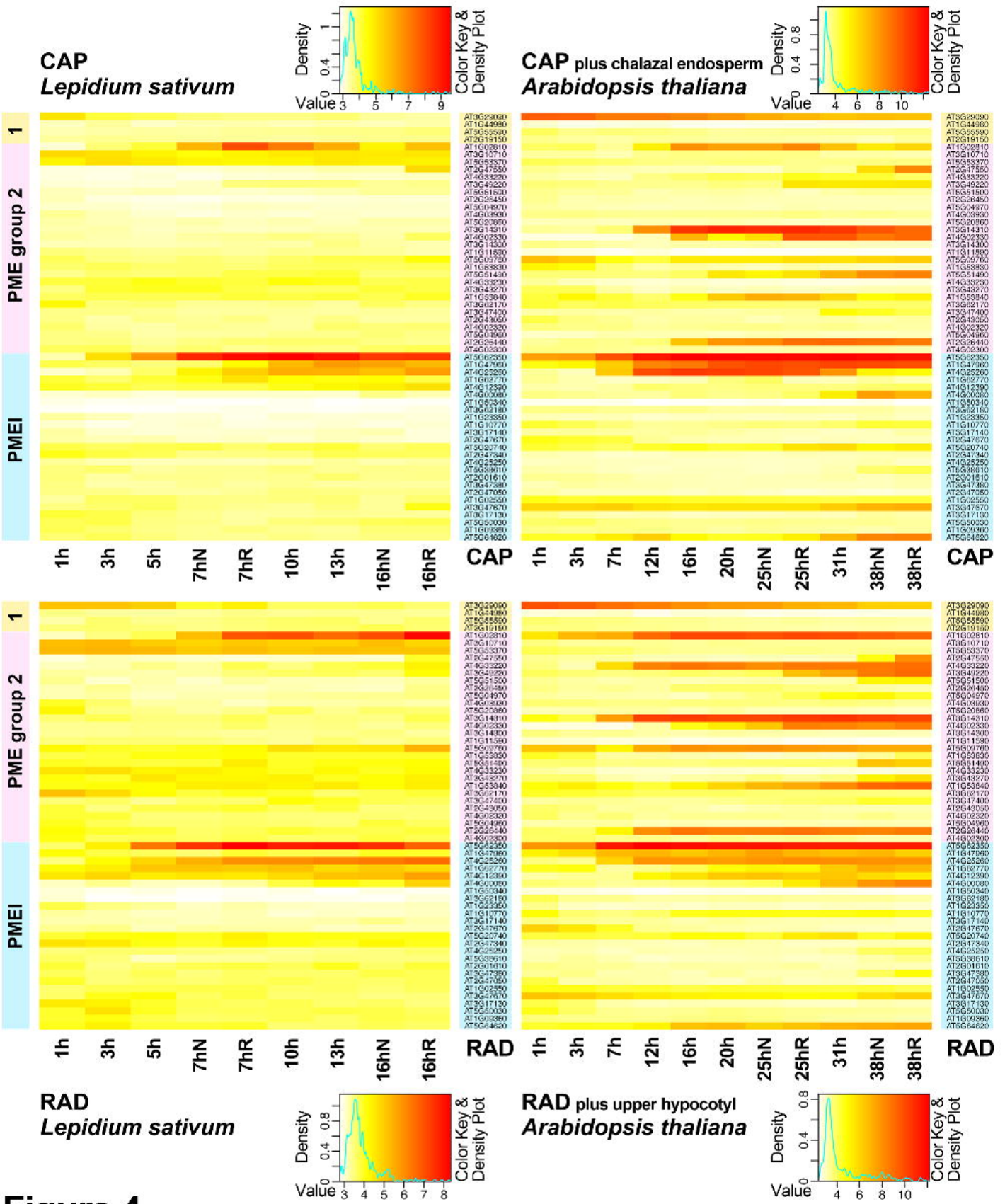

Figure 4. Seed compartment specific expression patterns of PMEs and PMEIs in Lepidium sativum and Arabidopsis. Top panels: Heat maps showing expression patterns of PME and PMEI transcripts in our microarrays of the L. sativum CAP (micropylar endosperm; left panel), compared to the expression of the putative Arabidopsis orthologue in the Arabidopsis MCE (CAP plus chalazal endosperm; right panel). Bottom panels: showing expression patterns of PME and PMEI transcripts in our microarrays of the L. sativum RAD (left panel), compared to the expression of the putative Arabidopsis orthologue in the Arabidopsis RAD (right panel). The Arabidopsis results were extracted from the microarray database published by Dekkers et al. (2013). Note that in contrast to L. sativum (Fig. 1B) the Arabidopsis "CAP compartment" contains the chalazal endosperm in addition to the micropylar endosperm, and the Arabidopsis "RAD compartment" contains upper hypocotyl in addition to the lower hypocotyl (embryo growth zone) and radicle (Dekkers et al., 2013).

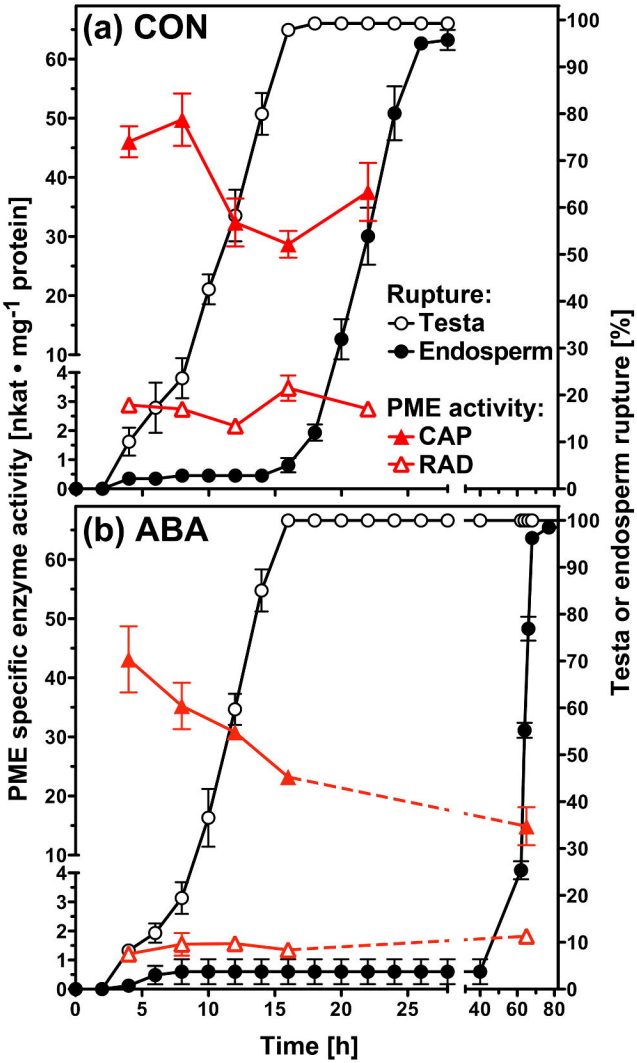

Figure 5. PME enzyme activity during the seed germination of Lepidium sativum. Seeds were imbibed in (A) water (CON, control) or (B) 5 µM abscisic acid (ABA). The kinetics of L. sativum testa rupture (TR) and endosperm rupture (ER) at 18°C in continuous light. PME enzyme activity was measured for protein extracts of CAP and RAD excised from imbibed seeds at the times indicated. Mean values ±SE for four biological replicates with 100 seeds each are presented.

(a)

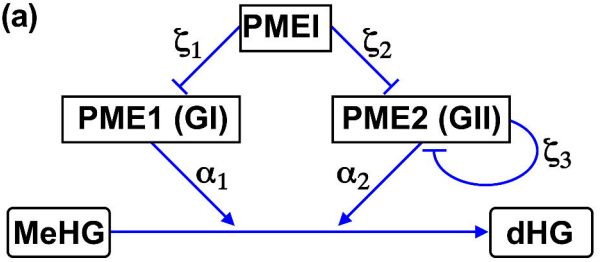

(b)

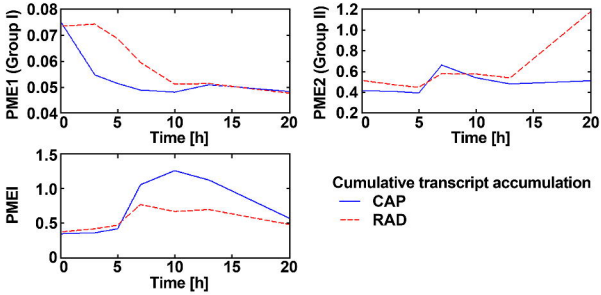

(c)

Ordinary Differential Equations (ODE) model

$$\frac{d[MeHG]}{dt} = -\alpha_1[G1][MeHG] - \alpha_2[G2][MeHG]. \quad (1)$$

$$\frac{d[dHG]}{dt} = \alpha_1[G1][MeHG] + \alpha_2[G2][MeHG]. \quad (2)$$

$$\frac{d[G1]}{dt} = -\zeta_1[G1][PMEI] + C\beta_{G1}(t) \quad (3)$$

$$\frac{d[G2]}{dt} = -\zeta_2[G2][PMEI] - \zeta_3[G2] + C\beta_{G2}(t) \quad (4)$$

$$\frac{d[PMEI]}{dt} = -\zeta_1[G1][PMEI] - \zeta_2[G2][PMEI] + C\beta_{PMEI}(t) \quad (5)$$

$$\frac{d[iG2]}{dt} = \zeta_3[G2] \quad (6)$$

$$\frac{d[PMEI:G1]}{dt} = \zeta_1[G1][PMEI] \quad (7)$$

$$\frac{d[PMEI:G2]}{dt} = \zeta_2[G2][PMEI] \quad (8)$$

(d)

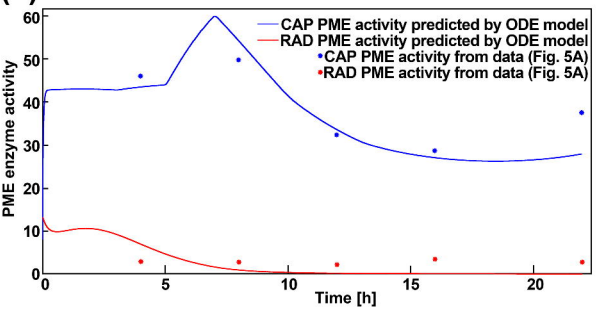

Figure 6. Mathematical model of contributions of group 1 PMEs, group 2 PMEs, and PMEIs to overall PME activity in RAD and CAP during *L. sativum* seed germination. **(A)** Network Diagram, where α_i are the rates at which MeHG is de-methylesterified and ζ_i the rates at which a PMEI domain binds with a PME domain. **(B)** Plots of the β functions: cumulative transcript levels for each group, within the CAP and RAD of *L. sativum* during germination; these levels are used as approximations of protein production. **(C)** Ordinary Differential Equations (ODE) based on our network model and the law of mass action. **(D)** Predicted PME activities when using the *L. sativum* PME model, and fitting to the *L. sativum* data (Fig. 5A) for PME enzyme activity within the CAP and the RAD. For a detailed description of the modelling see Materials and Methods, and for the parameter values for the mathematical model see Supplemental Table S3.

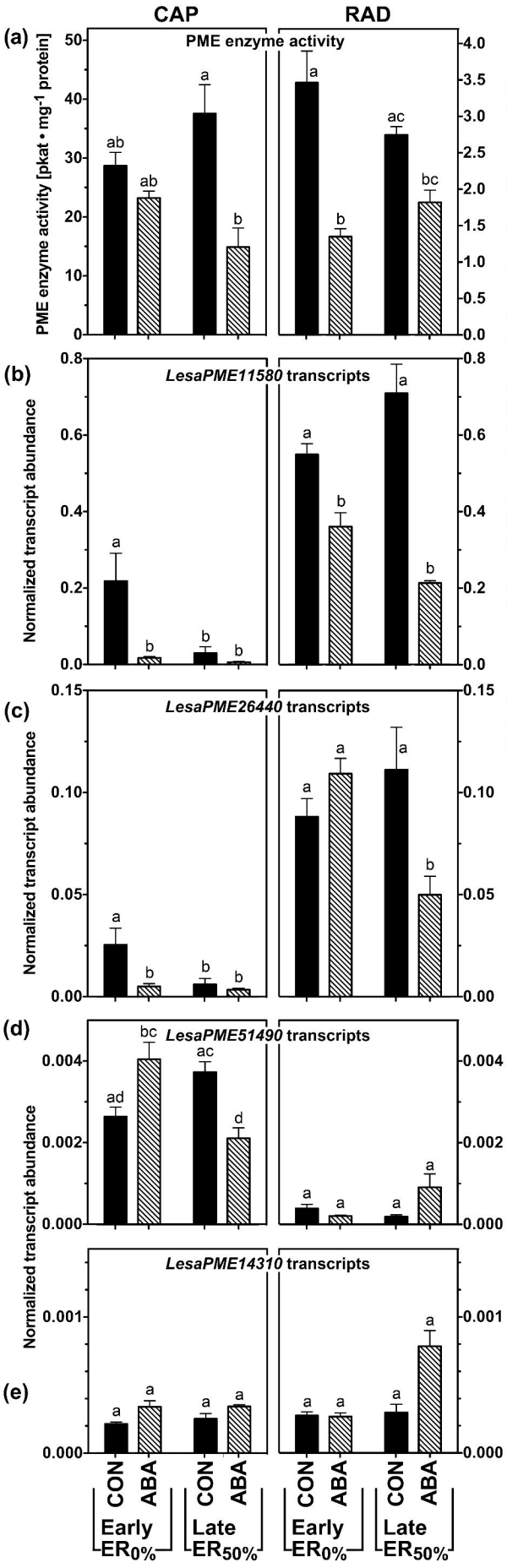

Figure 7.

Spatial and temporal analysis of transcript abundances of novel Lepidium sativum (Lesa) group 2 PMEs in germinating seeds (18ºC, continuous light) by quantitative RT-PCR. (A) PME enzyme activities as determined in Figure 5; note that scales for CAP and RAD are different. (B-E) Normalized transcript abundances of selected group 2 PMEs. Seeds were imbibed without (CON, control) or with ABA (5 µM). Micropylar endosperm (CAP) and the lower 1/3 of the radicle/hypocotyl axis (RAD) were excised from seeds; results for CAP (left) and RAD (right) are displayed on identical scales. Early germination: seeds after TR, but prior to ER (16 h). Late germination: seeds at ER50%, which was ca. 22 h for CON, ca. 65 h for ABA. Only unruptured CAPs were sampled. Lesa17210, Lesa04320 and Lesa20000 (Graeber et al. 2011) were used as references genes for the qRT-PCR normalization as described in the methods. Mean values ± SE for four biological replicates.

Statistical significance of CAP and RAD results were analysed separately by one-way ANOVA with Tukey's multiple comparison test performed using GraphPad Prism software (version 4.0 for Macintosh, GraphPad Software, San Diego California USA, www.graphpad.com). Mean values labelled with distinct letters differ significantly from each other with a P value <0.05.

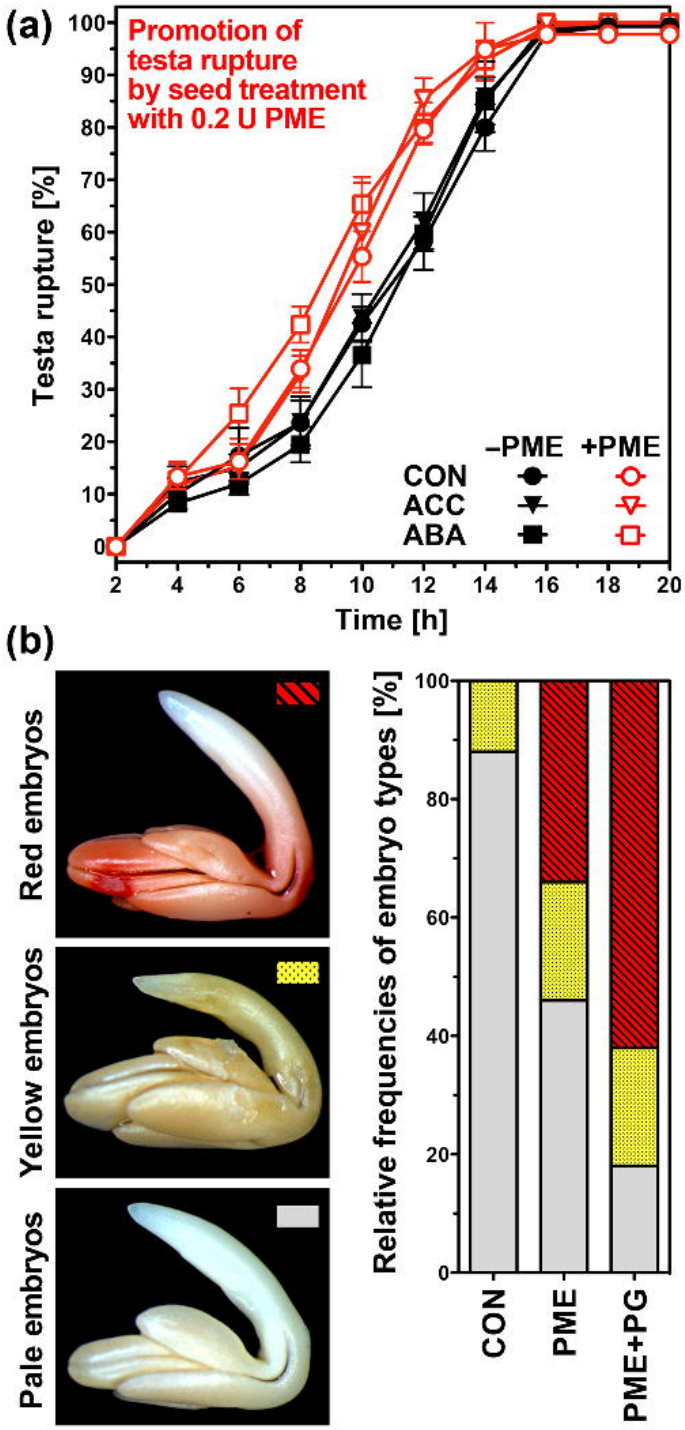

Figure 8. Treament of Lepidium sativum seeds with low amounts of PME promotes testa rupture and enhances testa permeability. (A) Treatment of imbibed seeds low amounts (0.2 U, i.e. 0.03 U/ml) of orange peel PME promoted but did not affect ER. This promotion of TR was by low PME amounts was not affected by simultaneous treatment with ABA or ACC. Note that in contrast to low amounts, relatively high amounts (ca. 20 U) of PME delayed TR and ER (Supplemental Fig. S6). Seeds were imbibed at 18ºC in continuous light; mean values ±SE of four biological replicates are shown. (B) Treatment of seeds with PME and pectin degradation by polygalacturonase (PG) enhances testa permeability as determined using the tetrazolium assay. Seeds were imbibed for 9h in tetrazolium salt assay solution without (CON) or with 0.2 U PME or PME+PG added. Embryos were excised and classified into five staining groups: pale (no staining, testa impermeable for tetrazolium salts), yellow (low testa permeability), and three categories of red (from partly to almost fully red, see Supplemental Fig. S7). Relative numbers based on 50 embryos for each series are presented. For different subcategories of red-stained embryos see Supplemental Fig. S7. Red embryo staining is indicative for increased testa permeability.